

Mineral equilibria at high PT-parameters

Bataleva Y.V.¹, Borzdov Y. M.¹, Palyanov Y.N.¹ Experimental modeling of the influence of reduced sulfur fluids UDC: 549.057; 549.322; 549.02

¹IGM SB RAS, Novosibirsk (bataleva@igm.nsc.ru, borzdov@igm.nsc.ru, palyanov@igm.nsc.ru)

Abstract. Experimental studies aimed at the evaluation the effect of reduced sulfur fluids on the processes of formation of diamond in assemblage with Fe³⁺-bearing magnesiowustite and pyrrhotite (or sulfide melt) were carried out in carbide-carbonate-sulfur system using the BARS apparatus (6.3 GPa, range of 900-1600 °C, 18-60 h). It was found that at 900 and 1000 °C, carbon is extracted from cohenite due to interaction with reduced sulfur fluid, and carbon-producing redox reactions of carbide with carbonate take place. At ≥ 1100 °C, the formation of an assemblage of Fe³⁺-magnesiowustite and graphite is accompanied by the generation of fO_2 -contrast melts - metal - sulfide with dissolved carbon (Fe-S-C) and sulfide with dissolved oxygen (Fe-S-O). It was found that the redox interaction of these melts, as well as the Fe-S-C melt and magnesiowustite, are carbon-producing processes accompanied by disproportionation of Fe and leading to the formation of an association of Fe³⁺-magnesiowustite, diamond and graphite. It has been experimentally demonstrated that the participation of sulfur fluids in diamond formation processes under subduction settings leads to an increase in the diamond crystallization temperature, a decrease in the diamond growth rate, and a sharp decrease in the partial melting temperature (~ 300 °C).

Keywords: diamond formation; sulfidation; sulfur-rich fluid; magnesiowustite; high-pressure experiment; lithospheric mantle; mantle metasomatism;

As an element sensitive to redox conditions, sulfur in the Earth's mantle can be found both in a reduced form (S²⁻ or S⁰ in sulfides, sulfide melts, or reduced fluid), and in an oxidized form (S⁶⁺ in sulfates, oxidized fluids, or dissolved in silicate melts) (Evans, 2012). Subduction processes play a key role in the transport of sulfur to the deep zones of the Earth; they are closely related to the global geochemical cycle of sulfur, the genesis of island arc sulfide ore deposits, and the evolution of the redox state of the mantle (Jégo, Dasgupta, 2014). In recent years, the behavior of sulfur in the processes of mantle metasomatism has been actively studied in relation to the genesis of sulfides in eclogites and peridotites of the subcontinental mantle (Alard et al., 2011). Taking into account the potential genetic relationship between diamond and sulfides (Bulanova, 1995; Palyanov et al., 2007; Bataleva et al., 2016), special attention should be paid to the assessment of the influence of sulfur-enriched metasomatic agents on the processes of diamond formation during the interaction of reduced mantle

rocks with the oxidized material of the subducting plate.

Experimental studies aimed at determining the role of reduced sulfur-enriched fluids in diamond formation processes under subduction conditions were carried out in the carbide-carbonate-sulfur system (Fe₃C-(Mg,Ca)CO₃-S) at a pressure of 6.3 GPa, in the temperature range of 900-1600 °C and durations of 18-60 hours. The results of interaction in simpler carbonate-metal and carbonate-carbide systems are detailed in (Palyanov et al., 2013). It has been experimentally established that at the lowest temperatures (900 and 1000 °C), pyrrhotite (Fe_{0.98-0.99}S), graphite, magnesiowustite (Fe_{0.69-0.75}Mg_{0.25-0.31}O) and aragonite, as well as recrystallized single crystals of the initial carbide and Mg,Ca-carbonates are formed in the carbide-carbonate-sulfur system. At the contact of the single crystals of cohenite, magnesite, and dolomite with newly formed pyrrhotite, the formation of reaction graphite rims (Fig.1a), similar to those described by us earlier (Bataleva et al., 2017) for the carbide-sulfur and carbide-sulfide systems, was established. It should be noted that magnesiowustite formed in this temperature range is homogeneous in composition within each sample and is always in assemblage with graphite, in the form of regular intergrowths, microcrystalline aggregates or inclusions. It was established by the Mössbauer spectroscopy that magnesiowustite contains ferric iron, with values of $Fe^{3+}/\Sigma Fe \sim 0.07$. At a temperature of 1100 °C in the carbide-carbonate-sulfur system, the formation of a solid-phase association pyrrhotite + magnesiowustite + graphite was established, as well as the formation of the first portions of Fe-S-C and Fe-S-O melts. In the range 1200-1600 °C, pyrrhotite is absent in the samples, and the phase association is represented by magnesiowustite, graphite (\pm diamond), and Fe-S-C and Fe-S-O melts (Fig. 1b). These melts in the samples are represented by quenching aggregates pyrrhotite + iron (with dissolved carbon) and pyrrhotite + wustite. The graphite in the samples is in intergrowths with magnesiowustite, and also forms "relict" reaction rims, denoting the boundaries of the crystals of the initial cohenite, which completely reacted during the experiments. Inside these graphite rims there are quenching aggregates of two melts (Fig. 1b). Depending on the temperature, the melts are characterized by the compositions of Fe₇₉S₂₀C₁ (1100 °C) - Fe₇₈S₁₉C₃ (1600 °C) and Fe₆₃S₃₅O₂ (1100 °C) - Fe₆₄S₃₀O₆ (1600 °C). Hereinafter, the compositions of the Fe-S-C and Fe-S-O melts are given in weight proportions (wt. %).

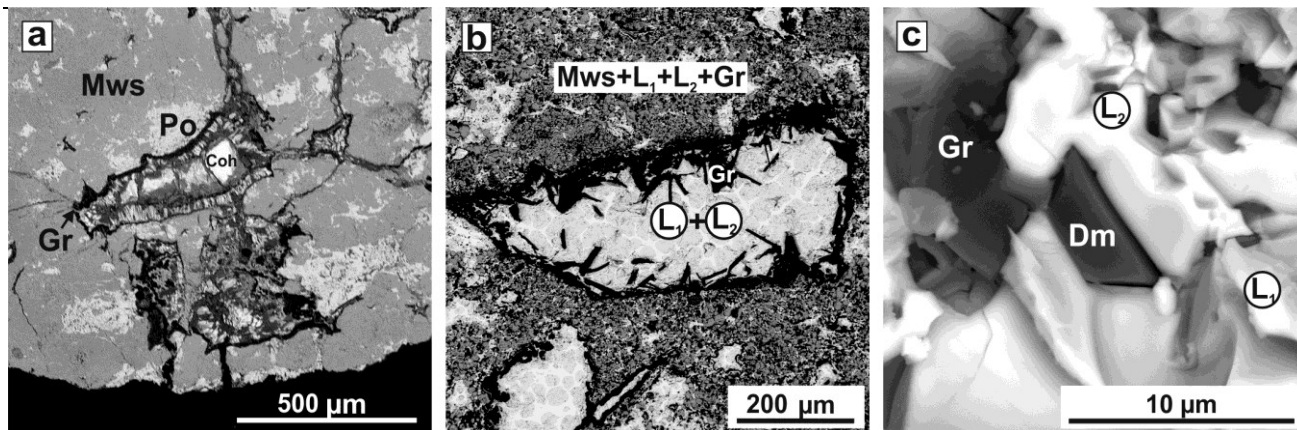


Fig. 1. SEM micrographs of polished fragments (a-b) and the cleavage surface of samples (c) obtained in the $\text{Fe}_3\text{C}-(\text{Mg,Ca})\text{CO}_3\text{-S}$ system at mantle P, T parameters: a - polycrystalline aggregate of magnesiowustite, graphite and pyrrhotite; in place of the original carbide crystals, a zonal aggregate is formed - cohenite (in the center) - pyrrhotite + high-ferrous carbonate - graphite border (900 °C); b - polycrystalline aggregate of magnesiowustite and graphite, in which there are segregations of quenched Fe-S-C melts in reaction rims of graphite (1200 °C); c - crystals of diamond and graphite in a quenched melt (1500 °C); Mws - magnesiowustite, L_1 - Fe-S-O melt, L_2 - Fe-S-C melt, Gr - graphite, Dm - spontaneously formed diamond, Po - pyrrhotite, Coh - cohenite;

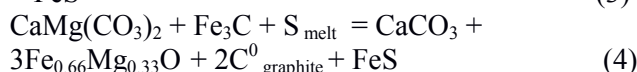
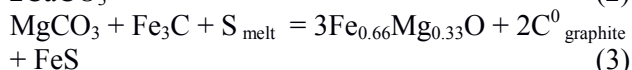
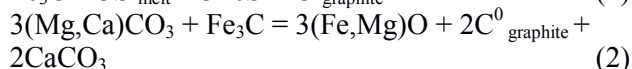
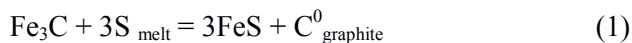
The composition of magnesiowustite in the range 1100-1500 °C is practically independent of temperature and corresponds to $\sim \text{Fe}_{0.64}\text{Mg}_{0.30}\text{Ca}_{0.06}\text{O}$, and the values of $\text{Fe}^{3+}/\sum\text{Fe}$ in it are at the level of 0.06-0.08. At a temperature of 1600 °C, the obtained magnesiowustite is represented by large rounded crystals with a zonal structure - a high-Mg center ($\sim \text{Fe}_{0.49}\text{Mg}_{0.46}\text{Ca}_{0.05}\text{O}$, $\text{Fe}^{3+}/\sum\text{Fe} \sim 0.07$) and a high-iron periphery ($\sim \text{Fe}_{0.93}\text{Mg}_{0.07}\text{O}$, $\text{Fe}^{3+}/\sum\text{Fe} \sim 0.12$).

The spontaneous formation of diamond as a result of the interaction of carbide-carbonate-sulfur, as well as the formation of an overgrown layer on diamond seed crystals, are established in the range of 1400-1600 °C. The resulting spontaneous diamond crystals are predominantly octahedra (5-80 μm), as well as their intergrowths (up to 120 μm). They are characterized by the presence of inclusions of magnesiowustite, and single inclusions of sulfide melt. Diamond crystals are located in a magnesiowustite + graphite polycrystalline aggregate, directly in contact with quenched Fe-S-C and Fe-S-O melts (Fig. 1c). The distribution of nucleation centers over the sample volume is uniform, and their number ranges from $\sim 10/\text{mm}^3$ (1400 °C) to $\sim 15/\text{mm}^3$ (1600 °C). The growth rate of spontaneous diamond crystals without taking into account the induction period is about 4-5 microns/hour.

It has been experimentally demonstrated that the processes of interaction in the system in the entire temperature range of 900-1600 °C occur with the participation of sulfur melt/fluid (Brazhkin et al., 1999). The behavior of this melt/fluid in the first approximation can be considered as a model for the behavior of a natural sulfur-rich reduced fluid - a powerful mantle metasomatic agent. Considering the previous results on the formation of diamond and graphite during redox interactions of iron carbide with Mg, Ca-carbonate (6.5-7.5 GPa, 1000-1650 °C,

Palyanov et al., 2013), it is possible to evaluate the effect of reduced sulfur fluid on these interactions.

It was found that at relatively low temperatures (900-1000 °C), the main processes of the formation of elemental carbon (graphite) during the interaction of carbide-carbonate-sulfur can be described by the following reactions:



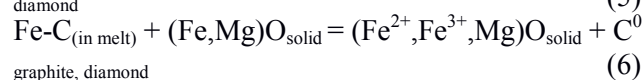
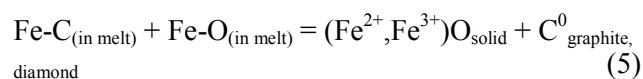
The interaction of cohenite with sulfur melt/fluid (1) is accompanied by the extraction of carbon and iron from carbide and leads to the formation of the pyrrhotite + graphite assemblage, as well as to the formation of graphite rims around the crystals of the initial Fe_3C . The features of this process are described in detail in (Bataleva et al., 2017). Redox reactions (2) - (4) describe the processes of carbon reduction of magnesite and dolomite upon interaction with cohenite, leading to the crystallization of graphite in association with magnesiowustite, pyrrhotite, and aragonite. It should be noted that graphite formed by reactions (2) - (4) is always spatially confined to magnesiowustite and is intergrown with it or is present in the form of inclusions, in contrast to graphite formed by reaction (1). In a simpler system $(\text{Mg,Ca})\text{CO}_3 - \text{Fe}_3\text{C}$ at 7.5 GPa and 1000-1100 °C (Palyanov et al., 2013), redox reactions of carbonate-cohenite take place with the formation of graphite, magnesiowustite and high-calcium carbonate, according to the reaction (2). Thus, as a result of the reconstruction of the processes of interaction of carbide-carbonate-sulfur under subsolidus conditions, it was found that the

main graphite-producing processes are the extraction of iron from cohenite upon interaction with the sulfur melt/fluid, as well as the reduction of carbonate carbon during the interaction with Fe₃C. It is most likely that at relatively low temperatures sulfur does not have a decisive effect on the crystallization of graphite by reactions (3) and (4), and its participation in them is limited to the crystallization of pyrrhotite, with a corresponding decrease in the iron content of magnesiowustite.

It was found that at temperatures above the solidus (≥1100 °C), the newly formed pyrrhotite melts, and the interaction of cohenite with the first portions of the sulfide melt occurs. As a result, the sulfide melt is enriched in iron and carbon, which leads to the formation of a Fe-S-C melt. In parallel with this process, the interaction of the sulfide melt with carbonate or carbonate melt also occurs, with the formation of the Fe-S-O melt and the solid-phase association magnesiowustite + graphite. The possibility of crystallization of graphite (or diamond) upon reduction of carbonate with Fe-S and Fe-S-O melts was previously demonstrated in (Gunn, Luth, 2006; Palyanov et al., 2007). Thus, the implementation of these processes under conditions of complete melting of sulfide leads to the formation of a single super-solidus phase association, represented by the melts Fe-S-C and Fe-S-O, Fe³⁺-bearing magnesiowustite and C⁰ (graphite and diamond).

Analysis of quenching aggregates of melts (using energy dispersive spectroscopy, scanning electron microscopy, Mössbauer spectroscopy) makes it possible to consider the Fe-S-O melt as a predominantly sulfide melt with dissolved FeO, the concentration of which in the melt, depending on the temperature, increases from 6 wt. % (1100 °C) up to 28 wt. % (1600 °C). In the Fe-S-C melt, on the contrary, the sulfide component is in a subordinate amount; it has been established that this melt is enriched in iron and carbon. The Fe-S-C melt obtained in the carbide-carbonate-sulfur system contains from 38 to 46 wt. % Fe⁰ and up to 3 wt. % of dissolved carbon. In other words, the interaction of carbide-carbonate-sulfur results in the generation of two melts contrasting in *f*O₂, one of which contains Fe²⁺ (FeO), and the other contains metallic iron. Despite the fact that in the samples obtained in this study, there are no reaction rims at the contact between the Fe-S-O and Fe-SC melts, direct evidence of their redox interaction is the crystallization of diamond and graphite directly in the Fe-S-C melt and the formation of enriched Fe²⁺ and Fe³⁺ rims of magnesiowustite in contact with the Fe-S-O melt. It should be noted that the crystallization of graphite and diamond is most likely carried out both as a result of the redox interaction between melts with the participation of magnesiowustite, which acts as a

Fe³⁺ concentrator phase, and during the interaction of the Fe-S-C melt with magnesiowustite directly, according to the following schemes:



This process of the formation of graphite and diamond, which occurs during the oxidation of the Fe-S-C melt with the Fe-S-O melt and/or magnesiowustite, can be considered as the basis for the reconstruction of the redox mechanism of diamond formation, which is realized as a result of the carbide-carbonate-sulfur interaction. It was found that under supersolidus conditions, diamond formation occurs in the Fe-S-C melt. Oxidation of the Fe-S-C melt by the Fe-S-O melt and/or magnesiowustite is accompanied by a decrease in the concentration of Fe⁰ in the Fe-S-C melt and the formation of magnesiowustite enriched in Fe²⁺ and Fe³⁺. This process leads to supersaturation of the Fe-S-C melt with carbon, which promotes the nucleation and growth of diamond. We assume that at the final stage of this process, when the Fe-C-component of the Fe-S-C melt is completely consumed, the phase composition of the samples will be represented by diamond, graphite, Fe³⁺-magnesiowustite, and sulfide melt.

Based on the comparison of the results obtained in the carbide-carbonate-sulfur systems with the results of the carbide-carbonate interaction (Palyanov et al., 2013), the main factors of the influence of the sulfur-enriched reduced fluid were revealed. In particular, this is a sharp decrease in the temperatures of partial melting and a decrease in the diamond-forming ability of the metal-carbon melt. In experiments with a redox gradient (Palyanov et al., 2013), aimed at studying the interaction of carbide-carbonate at 7.5 GPa and in the range of 1000-1400 °C, the formation of a solid-phase association cohenite + magnesiowustite + graphite was established in the reduced part of the samples. This work revealed and emphasized a direct relationship between the absence of spontaneous crystallization of diamond and the absence of the Fe-C melt. In the present study, it was found that the addition of 10.7 wt. % sulfur to the carbide-carbonate system leads to a decrease in the temperature of the beginning of partial melting of the system by at least 300 °C and the formation of the first portions of Fe-S-C and Fe-S-O melts at T = 1100 °C (6.3 GPa). Considering that the obtained Fe-S-C melt is a crystallization medium for graphite (1100-1600 °C) and diamond (1400-1600 °C), the data obtained can be considered when constructing natural models of diamond

formation in the presence of reduced sulfur metasomatic agents under subduction conditions.

Work is done on state assignment of IGM SB RAS.

References

- Alard O., Lorand J.-P., Reisberg L., Bodinier J.-L., Dautria J.-M., O'Reilly S. Volatile-rich metasomatism in Montferrier xenoliths (Southern France): Implications for the abundances of chalcophile and highly siderophile elements in the subcontinental mantle // *J. Petrol.* 2011. Vol. 52. P. 2009–2045.
- Bataleva Y.V., Palyanov Y.N., Borzdov Y.M., Bayukov, O.A., Zdrokov, E.V. Iron carbide as a source of carbon for graphite and diamond formation under lithospheric mantle P-T parameters // *Lithos.* 2017. Vol. 286-287. P. 151-161.
- Bataleva Y.V., Palyanov Y.N., Borzdov Y.M., Sobolev N.V. Sulfidation of silicate mantle by reduced S-bearing metasomatic fluids and melts // *Geology.* 2016. Vol. 44. I. 4. P. 271-274.
- Brazhkin V.V., Popova S.V., Voloshin R.N. Pressure-temperature phase diagram of molten elements: selenium, sulfur and iodine // *Phys. B Condens. Matt.* 1999. Vol. 265. P. 64–71.
- Bulanova G.P. The formation of diamond // *J. Geochem. Explor.* 1995. Vol. 53. P. 2–23.
- Evans K.A. The redox budget of subduction zones // *Earth Sci. Rev.* 2012. Vol. 113. P. 11–32.
- Gunn S.C., Luth R.W. Carbonate reduction by Fe-S-O melts at high pressure and high temperature // *Am. Miner.* 2006. Vol. 91. P. 1110-1116.
- Jégo S., Dasgupta R. The fate of sulfur during fluid-present melting of subducting basaltic crust at variable oxygen fugacity // *J. Petrol.* 2014. Vol. 55. P. 1019–1050.
- Palyanov Y.N., Bataleva Y.V., Sokol A.G., Borzdov Y.M., Kupriyanov I.N., Reutsky V.N., Sobolev N.V. Mantle–slab interaction and redox mechanism of diamond formation // *Proc. Natl. Acad. Sci. USA.* 2013. Vol. 110. I. 51. P. 20408-20413.
- Palyanov Y.N., Borzdov Y.M., Bataleva Y.V., Sokol A.G., Palyanova G.A., Kupriyanov I.N. Reducing role of sulfides and diamond formation in the Earth's mantle // *Earth Planet. Sci. Lett.* 2007. Vol. 260. I. 1-2. P. 242-256.

Burova A.I.^{1,2}, Chertkova N.V.², Spivak A.V.², Bobrov A.V.^{1,2,3}, Zakharchenko E.S.²
The phase relations in the ilmenite-olivine-H₂O system at a pressure of 6 GPa UDC 549.02

¹Geological Faculty, Moscow State University, Moscow, Russia, ²D.S. Korzhinskii Institute of Experimental Mineralogy RAS, ³Vernadsky Institute of Geochemistry and Analytical Chemistry RAS, Moscow, Russia

Abstract. The phase relations in the SiO₂-TiO₂-FeO-MgO-H₂O system have been studied experimentally at 6 GPa and 1200-1250°C. The following phases were found in the

experimental products: ilmenite, olivine and pyroxene. A phase reaction between the system components resulting in the formation of pyroxene was observed in the systems Ilm₁₈ – Ol₇₂-H₂O and Ilm₃₆ – Ol₅₄-H₂O. The obtained experimental data can be used to construct models of crystallization, growth and capture of H₂O-containing inclusions by diamond under conditions of high pressures and temperatures.

Keywords: *ilmenite, olivine, ice-VII, upper mantle, phase relations, high-pressure experiment*

Theoretical and experimental studies indicate that, under the conditions of the upper mantle, incorporation of water into rocks with a predominance of olivine is limited and only deeper horizons of the transition zone can be “water reservoirs” (Pearson et al., 2014). However, recent findings of ice-VII in inclusions in diamonds (together with ilmenite and also in association with olivine) (Tschauer et al., 2018) have shown that the remainder of the aqueous fluid crystallizes when the host diamonds rise.

In this regard, the determination of the phase relations in the ilmenite-olivine-water system at *PT*-parameters corresponding to the conditions of the Earth's upper mantle is of particular interest for studying diamond-forming systems and diamond formation in general. The main goal of this work is to study the phase relations in the Ilm-Ol-H₂O system under the conditions of the upper mantle and to reveal the phase relations. To achieve this goal, an experimental study of systems with the compositions (Pilm) Ilm-H₂O and (Pilm) Ilm-Ol-H₂O was performed using natural and model materials.

The experiments were carried out on a high pressure toroidal apparatus «anvil with hole» at IEM RAS, Chernogolovka. The pressure was generated by uniaxial compression of anvil with 13 mm holes on the working surfaces. The high-pressure cell was filled with gold "lenticular" ampoules, pre-filled with starting mixtures and soldered around the perimeter. The samples were subjected to a pressure of 6 GPa at temperatures of 1200-1250 ° C and kept for 60 minutes. The experiments were carried out with natural and model compositions of ilmenite. Picroilmenite powder from a kimberlite pipe named after V.I. Griba was used for experiments in a natural system, a synthetic mixture of Mg₂SiO₄ composition was used as the olivine component. In the model systems, the mixtures consisting of the components FeO and TiO₂ were applied. The starting mixtures were of a variable composition Mg₂SiO₄=90-x, FeTiO₃= x, H₂O=10 mol%, where x=72, 54, 36, 18.

The experimental samples were studied by electron microprobe analysis and Raman spectroscopy. Experimental conditions and results are shown in Tables 1 and 2.

Mineral equilibria at high PT-parameters

Table 1. Chemical and phase compositions of experimental samples of the microilmenite ± olivine-water system at 6 GPa.

№ sample	3250		3252		3253	
T, °C	1200		1250		1250	
Structure	Pilm ₈₆ – (H ₂ O) ₁₄		Pilm ₈₈ – (H ₂ O) ₁₂		(Pilm ₇₂ Ol ₁₈) – (H ₂ O) ₁₀	
Phase	<i>Pilm</i>	<i>rim'</i>	<i>Pilm</i>	<i>rim'</i>	<i>Ilm</i>	<i>ol</i>
SiO ₂	0,10	51,06	0,35		0,21	39,01
TiO ₂	56,35	3,39	56,17	4,28	58,32	2,24
Al ₂ O ₃	0,47	3,50	0,75	8,37	0,82	0,31
Cr ₂ O ₃	2,06	0,98	2,01	1,36	2,34	0,07
V ₂ O ₅	0,70	0,13	0,80	0,26	-	-
FeO	29,27	9,01	28,28	11,38	26,69	12,69
MgO	10,55	23,27	11,12	7,16	11,30	45,34
MnO	0,32	0,25	0,22	22,96	0,14	0,09
CaO	0,06	7,26	0,15	7,16	0,08	0,09
Na ₂ O	0,08	1,08	0,13	0,08	0,09	0,10
K ₂ O	0,02	0,06	0,03	43,24	0,02	0,08
Sum	100,00	100,00	100,00	100,00	100,00	100,00
Coefficients (f.u.)						
O	3		3		3	4
Si	0,00		0,01		0,00	0,97
Ti	0,98		0,97		1,00	0,04
Al	0,01		0,02		0,02	0,01
Cr	0,04		0,04		0,04	0,00
V	0,01		0,01		-	-
Fe	0,56		0,54		0,51	0,27
Mg	0,36		0,38		0,38	1,68
Mn	0,01		0,00		0,00	0,00
Ca	0,00		0,00		0,00	0,00
Na	0,00		0,01		0,00	0,01
K	0,00		0,00		0,00	0,00
Sum of cations	1,98		1,98		1,97	2,99

rim' – intergranular substance.

Table 2. Chemical and phase compositions of experimental samples of the ilmenite – olivine – water system at 6 GPa

№ sample	3260			3259			3262
T, °C	1250			1250			1250
Structure	Ilm ₁₈ Ol ₇₂ -(H ₂ O) ₁₀			Ilm ₃₆ Ol ₅₄ -(H ₂ O) ₁₀			Ilm ₇₂ Ol ₁₈ -(H ₂ O) ₁₀
Phase	<i>Ilm</i>	<i>ol</i>	<i>px</i>	<i>Ilm</i>	<i>ol</i>	<i>px</i>	<i>Ilm</i>
SiO ₂	0,00	39,16	56,69	0,00	39,94	54,77	0,00
TiO ₂	55,19	2,27	0,89	54,57	0,00	2,36	52,65
FeO	29,85	45,80	7,48	35,81	18,55	11,31	43,53
MgO	14,97	12,77	34,94	9,62	41,50	31,56	3,82
Sum	100,00	100,00	100,00	100,00	100,00	100,00	100,00
Coefficients (f.u.)							
O	3	4	6	3	4	6	3
Si	0,00	0,97	1,97	0,00	1,02	1,94	0,00
Ti	0,96	0,04	0,02	0,97	0,00	0,06	0,98
Fe	0,57	0,27	0,22	0,71	0,39	0,33	0,90
Mg	0,51	1,70	1,81	0,34	1,57	1,66	0,14
Sum of cations	2,04	2,98	4,01	2,03	2,98	4,00	2,02

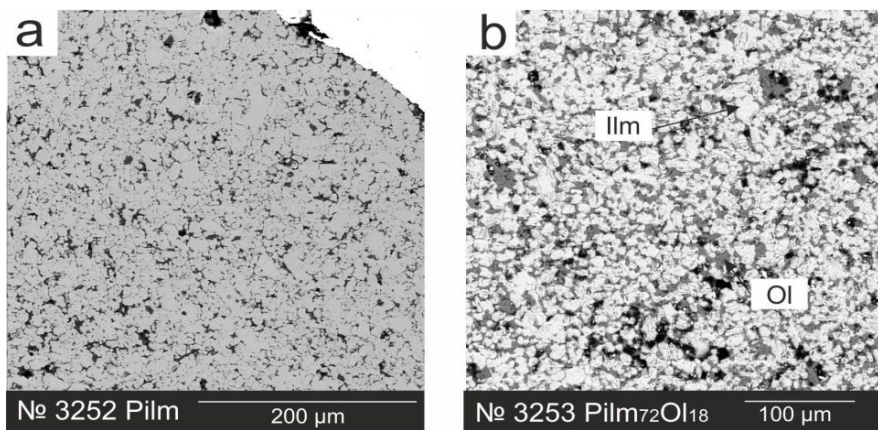


Figure 1. SEM images of the products of experiments obtained in the study of phase relations in systems: a - $\text{Pilm}_{90}\text{-H}_2\text{O}$; b - $\text{Pilm}_{72}\text{-Ol}_{18}\text{-H}_2\text{O}$;

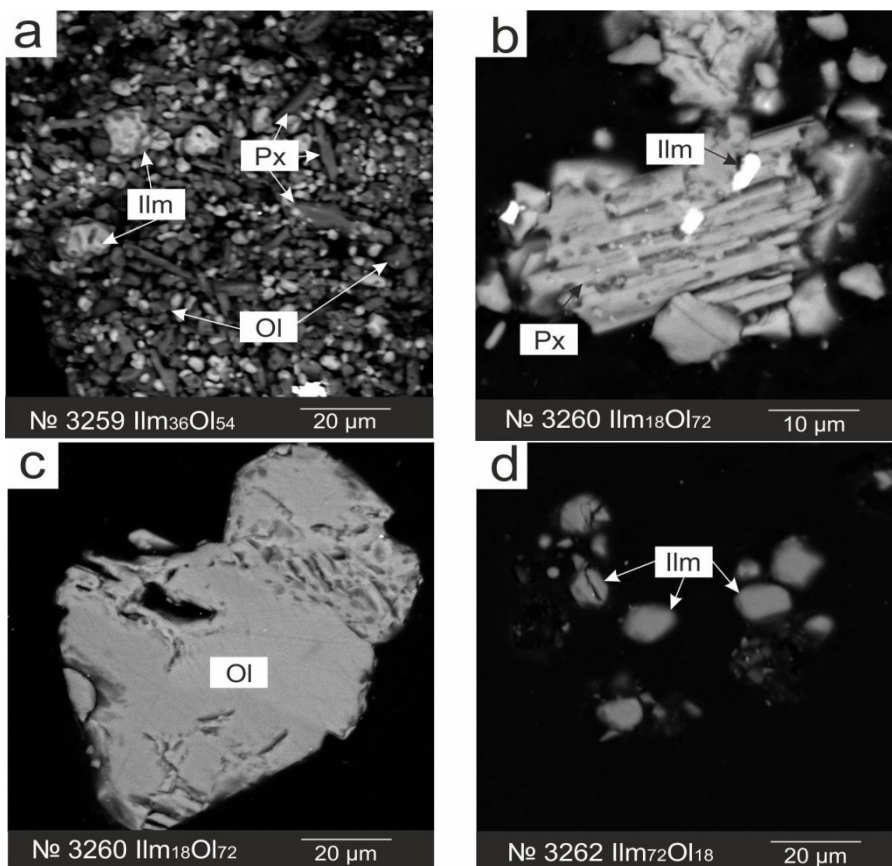


Figure 2. SEM images of the products of experiments obtained in the study of phase relations in systems: a – $\text{Ilm}_{36}\text{-Ol}_{54}\text{-H}_2\text{O}$; b,c – $\text{Ilm}_{18}\text{-Ol}_{72}\text{-H}_2\text{O}$; d – $\text{Ilm}_{72}\text{-Ol}_{18}\text{-H}_2\text{O}$.

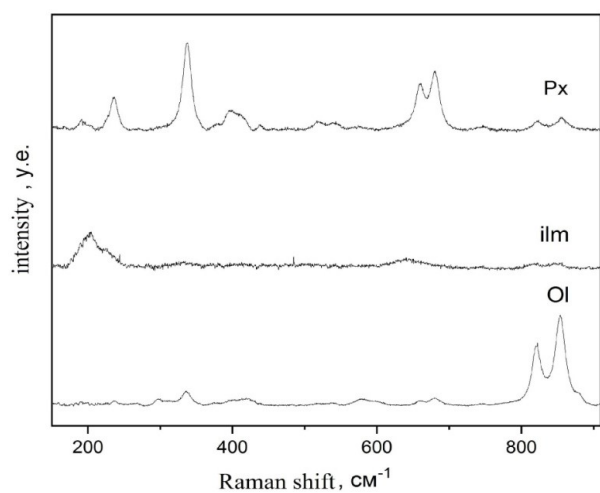


Figure 3. Raman spectra of pyroxene, ilmenite and olivine crystals obtained in the $\text{Ilm}_{36}\text{-Ol}_{54}\text{-H}_2\text{O}$ system

The following phases were found in the products of experiments: ilmenite, olivine, and pyroxene. Their amount and composition depends on the composition of the starting mixtures (Tables 1 and 2). In the natural Pilm-H₂O system (fig. 1a), the starting material underwent recrystallization. The intergranular substance (rim') has a non-stoichiometric composition, it acts as a concentrator of elements (Na, Mg, Al, Si, K) (Table 1), that are not incorporated into ilmenite structure. No reactions between picroilmenite and water were detected. With the addition of 18 mol% Mg₂SiO₄, two phases crystallize in the natural and model systems: olivine and ilmenite (Fig. 1b и 2d). Ilmenite forms continuous aggregate masses. Olivine is present in the form of small irregular grains, filling the space between the ilmenite crystals. An increased concentration of ferrous iron (FeO 12.69 mol%) is observed in the composition of olivine, and a titanium component is present as an impurity (TiO₂ up to 2.24 mol%) (Table 1).

With an increase in the content of the olivine component (Mg₂SiO₄) in the system, three phases are found among the products: ilmenite, olivine, and pyroxene (Fig. 2a-b). In the Ilm₃₆-Ol₅₄-H₂O system (Fig. 2a; Table 2), olivine together with ilmenite form the groundmass of the sample, composed of crystals up to 5 μm. However, some ilmenite crystals are larger up to 15 μm (Fig. 2a). Pyroxene grains are distinct from the groundmass because of their elongated appearance.

According to the results of microprobe analysis, olivine and pyroxene have significant contents of the iron component FeO (up to 18.55 mol% and 11.31 mol%, respectively) (Table 2). Titanium is present as an impurity in these phases. The Raman spectra of the three obtained phases are shown in Figure 3.

In the samples with the maximum content of the olivine component (Mg₂SiO₄=72 mol%), pyroxene (Fig. 2b) forms elongated grains up to 40 μm in size. Olivine is in the form of large crystals up to 100-150 microns, with irregular shape. These silicate phases are more ferrous compared to the products of experiments in the systems with a lower content of Mg₂SiO₄.

As a result of the experimental study, it was shown that reaction between water and ilmenite is not detected in the system without Mg₂SiO₄ component. However, with an increase in the content of the olivine component, a phase reaction occurs with the formation of pyroxene. The obtained experimental data can be used to construct models of crystallization, growth, and capture of H₂O - containing inclusions by diamond at high pressures and temperatures.

Acknowledgments: This work was carried out with the support of the Russian Science Foundation

(project No. 20-77-00079) and partially within the state task of the D.S. Korzhinskii Institute of Experimental Mineralogy of Russian Academy of Sciences (AAAA-A18-118020590140-7).

References

- Pearson, D., Brenker, F., Nestola, F. et al. Hydrous mantle transition zone indicated by ringwoodite included within diamond. *Nature* 507, 221–224 (2014). <https://doi.org/10.1038/nature13080>
- Tschauner O., Huang S., Greenberg E., Prakapenka, V. B., Ma C., Rossman G. R., Shen A. H., Zhang D., Newville M., Lanzirrotti, A., Tait K. (2018). Ice-VII inclusions in diamonds: Evidence for aqueous fluid in Earth's deep mantle. *Science*. 359. 1136-1139. [10.1126/science.aao3030](https://doi.org/10.1126/science.aao3030).

Butvina V.G.¹, Kosova S.A.¹, Safonov O.G.^{1,2}
Experimental study of the chromite-rutile / ilmenite-K₂CO₃-H₂O-CO₂ system at 2 GPa: an application to the mantle metasomatism
UDC 550.4.02

¹ IEM RAS, Chernogolovka (butvina@iem.ac.ru) ² Geol. faculty MSU, Moscow

Abstract. Formation of K-Na phases, where alkalis are bound to Cr, Ti, Fe³⁺, as a result of metasomatism in the upper mantle peridotites usually corresponds to later stages of metasomatic transformation. These phases are various K-Na-Ba-bearing titanates with a high chromium content, such as minerals of the mathiasite-lindsleyite and hawthorneite-yimengite groups and priderite. Experimental data on the stability of K-Ba-titanates are presented by a few works on their synthesis from mixtures of simple oxides and only limit the range of P-T conditions for their possible formation (Foley et al., 1994; Konzett et al., 2005). Our experiments showed a fundamental possibility of the formation of these titanates as a result of the reactions of chromite with aqueous- potassium carbonate fluids at 3.5 and 5 GPa and confirmed a wide range of existence of various titanates with respect to the fluid composition. Experiments at 2 GPa and 1000-1200°C showed that K-Cr priderite can crystallize in a wide range of temperatures and pressures (1.8-5 GPa) together with mathiasite, however, in a system rich in Fe (chromite-ilmenite-K₂CO₃-H₂O-CO₂), at pressures above 3.5 GPa, crystallization of yimengite and mathiasite is preferable.

Keywords: priderite, yimengite, rutile, chromite, ilmenite, aqueous carbonate fluid, potassium-carbonate, titanate, high pressure experiment, modal mantle metasomatism

Modal metasomatism is the most important process in the upper mantle, which determines not only the variety of assemblages of the mantle rocks, but also the formation of magmas specific in composition during their partial melting (Harte, 1983, etc.). Increased metasomatism, which is usually manifested by an increase of activity of alkaline components, leads to pyroxene reactions without the participation of Al-rich phases, leading, for example, to the formation of potassium richterite:

8En + Di + [1/2K₂O + 1/2Na₂O + H₂O] = KRich + 2Fo. The formation of other K-Na phases, where alkalis are bound to such components as Cr, Ti, Fe³⁺, in upper mantle peridotites usually correspond to even more advanced metasomatic transformations (Safonov, Butvina, 2016). These are a variety of K-Na-Ba-bearing titanates with a high chromium content, such as minerals of the mathiasite-lindsleite and hawthornite-imengite groups and priderite.

They are found mainly in metasomatized chromium-enriched peridotites in associations with phlogopite, potassium richterite, low-Al clinopyroxene, where garnet is absent (see Table 1 in Butvina et al., 2021), and spinel is characterized by high magnesium and chromium contents.

Experimental data on the stability of K-Ba-titanates (Fig. 1) are presented by a few works on their synthesis from mixtures of simple oxides and only limit the range of P-T conditions for their possible formation (Foley et al., 1994; Konzett et al., 2005). They do not reproduce the actual reactions of the formation of these minerals in mantle assemblages caused by the action of alkali-rich fluids/melts on Cr and Ti-bearing peridotite minerals. Our experiments (Butvina et al., 2019, 2020) showed the fundamental possibility of the formation of these titanates as a result of reactions of chromite with aqueous-potassium carbonate fluids at 5 GPa and confirmed the wide range of the existence of various titanates with respect to the composition of the fluid.

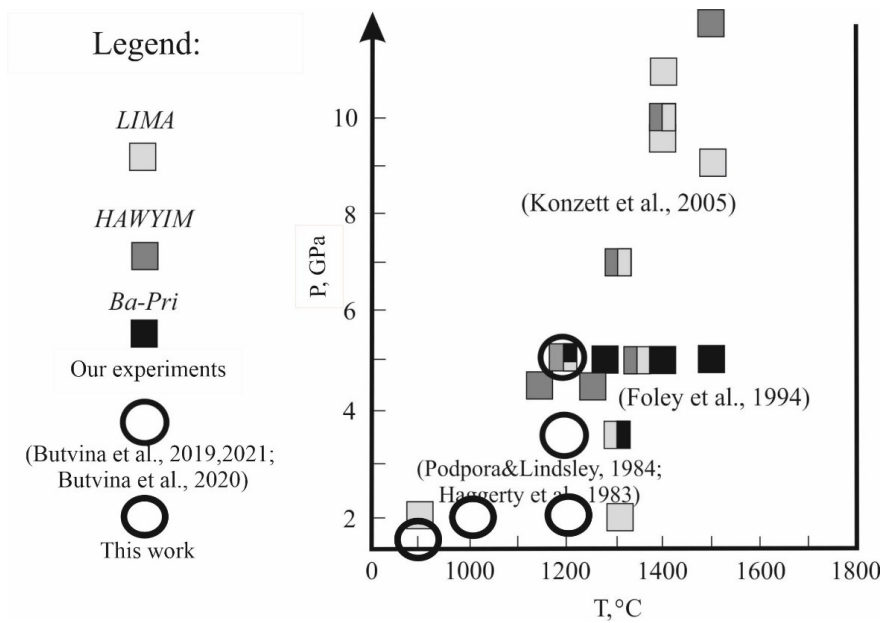


Fig. 1. Available data on the synthesis of K-titanates from oxides under various PT conditions.

Thus, phlogopite and titanates are minerals that are indicative of extreme manifestations of mantle metasomatism at its initial and most advanced stages. The purpose of this article is to summarize the previously obtained and new experimental data on the study of metasomatic reactions of the formation of chromium-containing potassium titanates of the crichtonite, magnetoplumbite and hollandite groups with the participation of H₂O-(CO₂)-KCl and H₂O-(CO₂)-K₂CO₃ fluids at 1.8-2.0 GPa and 900-1200°C. The experiments were carried out using a piston-cylinder apparatus at the IEM RAS (Chernogolovka, Moscow region).

Starting materials. In experiments on the reactions of the formation of potassium titanates, natural chromite was used as a starting component (Butvina et al., 2021), which was mixed with a powder of synthetic TiO₂ or natural ilmenite in the ratios of 1:1 or 2:1:1 by weight. Chromite of the composition (Mg_{0.49-0.54}Fe_{0.50-0.54}Mn_{0.01-0.02}Zn_{0.01-0.02})(Al_{0.17-0.20}Cr_{1.55-1.61}Fe_{0.10-0.22}Ti_{0.03-0.07})O₄ was

selected from a garnet lherzolite xenolith from the Pionerskaya kimberlite pipe, Arkhangelsk province. Ilmenite of the composition Fe_{0.98}Mg_{0.01}Mn_{0.06}Ti_{0.93}Al_{0.01}Nb_{0.01}O₃, is a xenocrystal from kimberlite of the Udachnaya Tube, Yakutia. A mixture of K₂CO₃ (+KCl) and oxalic acid in the ratios of 9:1 by weight was used as the fluid component. The chromite + TiO₂ mixtures were mixed with a "fluid" mixture in a ratio of 9:1 by weight. See Table 1 for the experimental conditions and results.

Discussion. The presence of priderite and mathiasite was confirmed by Raman spectroscopy. The Raman spectra are indistinguishable from those obtained earlier (see Butvina et al., 2019, 2020, 2021). The conducted experiments show that the associations of potassium titanates can be indicators not only of potassium activity in the processes of mantle metasomatism, but also indicators of Fe, as well as pressure during this process. Cr-bearing priderite was not detected in the chromite-ilmenite-

K₂CO₃-H₂O-CO₂ system at 3.5 GPa, but it actively crystallizes in the chromite-**rutile**-K₂CO₃-H₂O-CO₂ system at 5 GPa, together with mathiasite. At a pressure of 1.8-2.0 GPa, priderite is intensively formed in all systems, its synthesis together with mathiasite occurs only in an Fe-rich system in the presence of ilmenite.

Yimengite does not form at such pressures, the formation of priderite and mathiasite is preferable. 1. It is shown that the synthesis of yimengite was not carried out below 5.0 GPa, however, in our earlier works it was shown that at 3.5 GPa yimengite is intensively formed in the chromite-ilmenite-K₂CO₃-H₂O-CO₂ system, accounting for more than 25% of the obtained sample (Butvina et al., 2021). It is known that priderite (in contrast to the minerals of the crichtonite and magnetoplumbite groups) is both a typical matrix mineral of leucite lamproites (Prider, 1939; Jaques et al., 1989; Jaques, 2016), and is found as inclusions in diamonds (Jaques et al., 1989). This indicates a wide pressure interval of crystallization of priderite. This is also indicated by the experiments of

Foley et al. (1994), where priderite crystallized at both 5 GPa and 3.5 GPa (Fig.1).

However, the crystallization of Cr-free Fe³⁺ and Fe²⁺-priderite, characteristic of lamproites, was studied in experiments. The chromium-dominant variety of priderite is formed exclusively in metasomatized peridotite xenoliths (Haggerty 1991; Konzett et al., 2014; Giuliani et al., 2012). Jaques et al., (1989) specifically note that Cr-rich (up to 8 wt. % Cr₂O₃) priderite was detected only in the heavy fraction of lamproites, reflecting the mineral composition of disintegrated xenoliths. We first crystallized K-Cr priderite (Butvina et al., 2019), further work, as well as this article, shows that K-Cr priderite can crystallize in a wide range of temperatures and pressures (1.8-5 GPa) together with mathiasite, however, in a system rich in iron (chromite-**ilmenite**-K₂CO₃-H₂O-CO₂), at a pressure above 3.5 GPa, the crystallization of yimengite and mathiasite is preferable (Butvina et al., 2021; Butvina et al., 2020).

Table 1. Conditions and results of experiments on the synthesis of K-Cr titanates at 1.8-2.0 GPa.

No№	Mineral composition (mass.%)	Fluid, (mas.%)	Fluid content in the system, %	Time, h.	T, °C; P, GPa	Synthesis of priderite, yimengite, mathiasite, phlogopite; etc.
Ma-1	Spinel: rutile (1:1)	K ₂ CO ₃ :o.a.* (9:1)	10	48	1200; 2.0	-,-,-; availability of the source material
Ma-2	Spinel: ilmenite (1:1)	K ₂ CO ₃ :o.a. (9:1)	10	48	1200; 2.0	+,-,+
Ma-3	Spinel: rutile (1:1)	K ₂ CO ₃ :o.a. (9:1)	10	48	1000; 2.0	ampoule ejection
Ma-4	Spinel: ilmenite (1:1)	K ₂ CO ₃ :o.a. (9:1)	10	48	1000; 2.0	+,-,+,-
Ma-5	Spinel: rutile (1:1)	KCl:K ₂ CO ₃ :o.a. (4.5:4.5:1)	10	96	1000; 2.0	+,-,-,-
Ma-6	Spinel: ilmenite (1:1)	KCl:K ₂ CO ₃ :o.a. (4.5:4.5:1)	10	96	1000; 2.0	+,-,+,-
Ma-7	Spinel: ilmenite: rutile (2:1:1)	K ₂ CO ₃ :o.a. (9:1)	10	96	900; 1.8	+,-,+,-

*oxalic acid.

Conclusions. The experimental results presented in this article are simulations of reactions representing various stages of potassium metasomatism of peridotites in the conditions of the subcontinental lithospheric mantle. The initial stages of this process are expressed in the modification of the mineral compositions of the original peridotites during the reactions of the formation of phlogopite. The progress of further transformations leads to the formation of other potassium minerals. These are, in particular, potassium titanates. Experiments on the formation of yimengite, mathiasite and priderite in the chromite – rutile/ilmenite - K₂CO₃ – H₂O-CO₂

system at 1.8, 2.0, 3.5 and 5 GPa proved the fundamental possibility of the formation of these minerals during the reactions of chromite with the aqueous-potassium carbonate fluid. The formation of these minerals follows the formation of phlogopite, and also requires an additional source of titanium, i.e. rutile and ilmenite, which themselves are usually products of modal metasomatism of peridotites.

The assemblages of titanates with phlogopite characterize a higher activity of the potassium component in the fluid/melt than the formation of phlogopite alone. Such conditions can be imposed at the most progressive stages of the mantle

metasomatism. So, the experiments confirm that the formation of titanates is associated with repeated stages of metasomatism in mantle peridotites with an increasing effect. Relations between titanates is also a function of the activity of the potassium component in metasomatizing fluids/melts and, possibly, pressure. Examples from natural assemblages of metasomatized peridotites well illustrate the conclusions from the experiments. They also suggest new tasks for the experiments, which consists in reproduction of physico-chemical conditions and reactions in a single series of experiments simulating the transformation of garnet peridotites from the initial phlogopite-forming reactions to the formation of additional potassium phases, including potassium titanates.

The work was carried out within the framework of the topics AAAA18-118020590140-7 and AAAA18-118020590148-3 of the state task of the IEM RAS for 2021-2023

References

- Butvina V. G., Vorobey S. S., Safonov O. G., Varlamov D. A., Bondarenko G. V., Shapovalov Yu. B. (2019) Experimental study of the formation of chromic pryderite and imengite-products of modal mantle metasomatosis. *DAN* 486 (6), 709-713 (Russian)
- Butvina V. G., Safonov O. G., Vorobey S. S., Limanov E. V., Van K. V., Bondarenko G. V., Garanin V. K. Experimental study of reactions of formation of phlogopite and potassium titanates-indicator minerals of metasomatosis in the upper mantle. *Geochemistry* 66(8):709-730 (Russian)
- Safonov O. G., Butvina V. G. (2016) Reactions-indicators of K and Na activity in the upper mantle: natural and experimental data, thermodynamic modeling. *Geochemistry* 10, 893-908 (Russian)
- Butvina V.G., Vorobey S.S., Safonov O.G., Bondarenko G.V. (2020) Formation of K-Cr titanates from reactions of chromite and ilmanite/rutile with potassic aqueous-carbonic fluid: experiment at 5 GPa and applications to the mantle metasomatism. *Springer Nature* 9, 201-222.
- Foley S., Hofer H., Brey G. (1994). High-pressure synthesis of priderite and members of lindsleyite-mathiasite and hawthorneite-yimengite series. *Contrib. Mineral. Petrol.* 117, 164-174.
- Giuliani A., Kamenetsky V.S., Phillips D., Kendrick M.A., Wyatt B.A., Goemann K. (2012) Nature of alkali-carbonate fluids in the sub-continental lithospheric mantle. *Geology* 40 (11), 967-970.
- Haggerty S. E., Smyth J. R., Erlank A. J., Rickard R.S., Danchin R. V. (1983) Lindsleyite (Ba) and mathiasite (K): two new chromium-titanates in the crichtonite series from the upper mantle. *Am Mineral*, 68, 494-505.
- Haggerty S.E. (1991) Oxide mineralogy of the upper mantle. (Eds. Lindsley D.H.). *Oxide Minerals: Petrologic and Magnetic Significance. Reviews in Mineralogy*, 25, 355– 416.
- Harte B. (1983) Mantle peridotites and processes—The kimberlite sample. (Eds. Hawkesworth C.J., Norry M.J.) In: *Continental Basalts and Mantle Xenoliths*, Shiva: Cheshire, UK, 46–91.
- Jaques A.L., Hall A.E., Sheraton J.W., Smith C.B., Sun S.S., Drew R.M., Foudoulis C., Ellingsen K. (1989) Composition of crystalline inclusions and C-isotopic composition of Argyle and Ellendale diamonds. In: *Kimberlites and related rocks 2: their crust/mantle setting, diamonds, and diamond exploration.* (Eds. Jaques A.L., Ferguson J., Green D.H.) Blackwells, Melbourne, 966-989.
- Jaques A.L. (2016) Major and trace element variations in oxide and titanate minerals in the West Kimberley lamproites, Western Australia. *Mineral Petrol*, 110, 159–197.
- Konzett J., Yang H., Frost D.J. (2005) Phase relations and stability of magnetoplumbite- and crichtoniteseries phases under upper-mantle P-T conditions: an experimental study to 15GPa with implications for LILE metasomatism in the lithospheric mantle. *J. Petrol.* 46 (4), 749-781.
- Konzett J., Krenn K., Rubatto D., Hauzenberger C., and Stalder R. (2014) The formation of saline mantle fluids by open-system crystallization of hydrous silicate-rich vein assemblages—Evidence from fluid inclusions and their host phases in MARID xenoliths from the central Kaapvaal Craton, South Africa. *Geochim. Cosmochim. Acta* 147, 1–25.
- Podpora, C., Lindsley, D. H. 1984. Lindsleyite and mathiasite: synthesis of chromium-titanates in the crichtonite (AlM₂O₃8) series. *EOS Transactions, American Geophysical Union* 65, 293.
- Prider R. T. (1939) Some minerals from the leucite-rich rocks of the west Kimberley area, Western Australia. *Min. Mag.* 25, 373-387.

Furman O.V.^{1,2}, Bataleva Yu.V.¹, Borzdov Yu.M.¹, Palyanov Yu. N.^{1,2}. Experimental study of the influence of sulfur concentration on the olivine sulfidation at high pressure and temperature. UDC 549.057

¹Sobolev Institute of Geology and Mineralogy, Siberian Branch of the Russian Academy of Sciences, Novosibirsk, ²Novosibirsk State University, Novosibirsk (furmano@igm.nsc.ru, bataleva@igm.nsc.ru, borzdov@igm.nsc.ru, palyanov@igm.nsc.ru)

Abstract: Experimental studies aimed at the modeling of the interaction processes of sulfur metasomatic agents with mantle silicates and estimation of the effect of sulfur content on the sulfidation of olivine were carried out in the system Fe, Ni-olivine + sulfur on multi-anvil high-pressure apparatus of a split sphere type (BARS) (1050 and 1450 °C, 6.3 GPa, 40-60 hours, sulfur concentration in the system (Xs) 0.1, 2, and 6 mol%). It was found that as a result of recrystallization of Fe, Ni-olivine in the sulfur melt, Fe and Ni are extracted from olivine into this melt and crystallization of Fe, Ni-sulfides and low-iron silicates as independent phases is realized. With an increase in Xs, a regular increase in the amount of newly formed sulfides and silicates occurs, accompanied by a decrease in the contents of FeO and NiO in olivine and the newly formed orthopyroxene. A new mechanism for sulfidation of iron-bearing silicates in the mantle under the influence of sulfur as a component of reduced deep fluid is disclosed. It has been experimentally demonstrated that reducing agents of

sulfur metasomatism, even at minimal concentrations, are able to dissolve and transport mantle silicates and sulfides, as well as play one of the key roles in ore-forming processes involving mantle sulfur fluids.

Keywords: mantle metasomatism; mantle fluid; olivine sulfidation; reduced sulfur fluid; high-pressure experiments

Introduction. The study of the processes of mantle metasomatism is one of the most actual directions of mantle petrology at present. Sulfur fluids, sulfide melts, and reduced components of C-O-H fluid, for example, CH₄, are considered as potential agents of reducing mantle metasomatism (O'Reilly and Griffin, 2013). At the same time, the main sources of sulfur-bearing melts and fluids in the mantle are crustal material immersed in the subduction zone, fluid flows from the core-mantle boundary, and mantle plume material (Evans, 2012; Tomkins, Evans, 2015). When these sulfur fluids or melts act on iron- and nickel-bearing silicates of mantle rocks, the so-called sulfidation reactions occur. Most of the currently available experimental studies related to the sulfidation of olivine were carried out at atmospheric pressure, as well as with the use of ferrous olivine - fayalite:

$2\text{FeMgSiO}_4 + 3\text{S} \rightarrow 2\text{FeS} + 2\text{MgSiO}_3 + \text{SO}_2$ [1974 atm, 800 °C] (Kullerud, Yoder, 1963)

$\text{Mg}_2\text{SiO}_4 + 0,5\text{S}_2 + \text{C} \rightarrow \text{MgSiO}_3 + \text{MgS} + \text{CO}$ [1 atm, 1200 °C] (Fleet, MacRae, 1987)

$\text{Fe}_2\text{SiO}_4 + \text{S}_2 \rightarrow 2\text{FeS} + \text{O}_2 + \text{SiO}_2$ [Lodran achondrite study] (Papike et al., 1995)

$(\text{Mg,Fe,Ni})_2\text{SiO}_4 + \text{S}_{\text{liq}} \rightarrow \text{MgSiO}_3 + \text{Mg}_2\text{SiO}_4 + (\text{Fe,Ni})\text{S}_2 + (\text{S-Fe-Ni-O-Si-Mg})_{\text{liq}}$
[6.3 GPa, 1050-1450 °C] (Bataleva et al., 2016)

Yu.V. Bataleva et al. (2016) studied the interaction processes in the Fe, Ni-bearing olivine - sulfur system, while the sulfur concentration was constant and relatively high (10 mol%). This experimental study is a logical continuation of the work (Bataleva et al., 2016), and is aimed at studying

the effect of various sulfur concentrations on olivine sulfidation.

Experiments were carried out at a pressure of 6.3 GPa, temperatures of 1050 and 1450 °C, durations of 40 and 60 hours, on multi-anvil high-pressure apparatus of a split sphere type (BARS). Sulfur concentrations in the systems were 0.1, 2, and 6 mol%. Forsterite from xenolith of spinel lherzolite from the Udachnaya pipe and elemental chemically pure sulfur were used as starting materials. The composition of the initial olivine is Mg_{1.8}Fe_{0.19}Ni_{0.01}SiO₄. MgO content of initial olivine is 49.34 wt%, FeO - 9.28 wt%, NiO - 0.51 wt%, SiO₂ - 40.87 wt%.

Results of relatively low-temperature experiments (1050 °C). Using a complex of analytical methods it was established that at sulfur concentration of 0.1 mol%, a polycrystalline olivine aggregate is formed, with single crystals of newly formed nickel sulfide and orthopyroxene (**Fig.1a**). The composition of olivine practically does not differ from the initial one (**Fig.2, Table 1**). At 2 mol% sulfur, an assemblage of recrystallized olivine with a zonal structure and sulfide inclusions was obtained, while numerous small crystals of sulfides and orthopyroxene were found in the interstices (**Fig.1b**). The profiles of zoned olivine crystals demonstrate a decrease in the FeO concentration in the rims to 5 wt% (**Fig.2**). At the highest sulfur concentrations, the formation of an association of recrystallized olivine, newly formed orthopyroxene and pyrite, coexisting with predominantly sulfur melt, was established (**Fig.1c, Table 1**).

As a result of the reconstruction of olivine sulfidation processes, it was found that at a relatively low temperature (1050 °C) following processes occur: (1) recrystallization of olivine in a sulfur melt; (2) partial extraction of Fe and Ni from olivine into a sulfur melt; (3) formation of sulfide inclusions in olivine; (4) crystallization of newly formed sulfides; (5) formation of newly formed orthopyroxene; (6) decrease in the iron content of olivine.

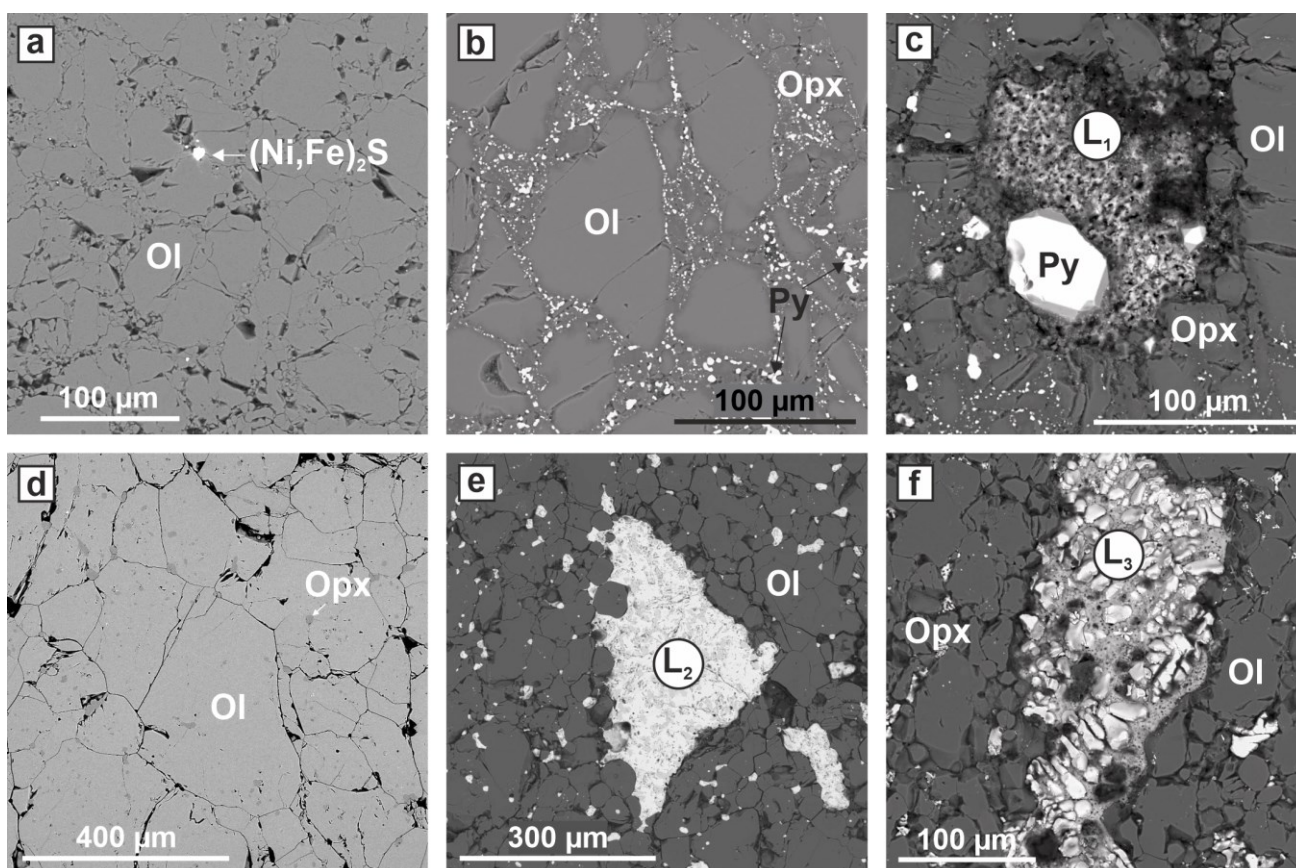


Fig.1. SEM micrographs of polished samples surfaces:

a - polycrystalline olivine aggregate ($T = 1050\text{ }^{\circ}\text{C}$, $X_s = 0.1\text{ mol\%}$); b - polycrystalline aggregate of recrystallized olivine, newly formed sulfides and orthopyroxene ($T = 1050\text{ }^{\circ}\text{C}$, $X_s = 2\text{ mol\%}$); c - polycrystalline aggregate of olivine and orthopyroxene with quenched sulfur melt ($T = 1050\text{ }^{\circ}\text{C}$; $X_s = 6\text{ mol\%}$); d - polycrystalline aggregate of olivine and newly formed orthopyroxene ($T = 1450\text{ }^{\circ}\text{C}$, $X_s = 0.1\text{ mol\%}$); e - polycrystalline aggregate of recrystallized olivine with sulfide inclusions and quenched sulfide melt ($T = 1450\text{ }^{\circ}\text{C}$, $X_s = 2\text{ mol\%}$); f - polycrystalline aggregate of olivine and orthopyroxene with quenched sulfur-sulfide melt ($T = 1450\text{ }^{\circ}\text{C}$; $X_s = 6\text{ mol\%}$). Ol - olivine, Opx - orthopyroxene, Py - pyrite, L_1 - sulfur melt, L_2 - sulfide melt, L_3 - sulfur-sulfide melt.

Table 1. Compositions of silicates

Run N	T, $^{\circ}\text{C}$	Xs, mol%	Phase	Composition, wt%				
				SiO ₂	FeO	MgO	NiO	Total
930/7-A1	1050	0.1	Ol	40.7	9.2	49.5	0.5	99.9
			Opx	58.3 ₍₆₎	6.3 ₍₂₎	34.8 ₍₄₎	-	99.4
930/7-A2	1050	2	Ol	41.2	6.7	51.7	0.2	99.9
			Opx	58.6 ₍₈₎	3 ₍₂₎	37 ₍₂₎	-	99.5
930/7-A3	1050	6	Ol	43.2	4.2	52.1	0.4	99.9
			Opx	58.4 ₍₈₎	5 ₍₂₎	36 ₍₁₎	-	99.7
929/7-A1	1450	0.1	Ol	40.7	8.6	50.1	0.5	99.9
			Opx	57.8 ₍₆₎	6.0 ₍₁₎	35.0 ₍₃₎	-	98.8
929/7-A2	1450	2	Ol	42.4	2.9	54.7	-	100.0
			Opx	58.8 ₍₅₎	2.0 ₍₃₎	38.2 ₍₃₎	-	99.0
929/7-A3	1450	6	Ol	43.0	0.4	56.5	-	99.1
			Opx	59.3 ₍₅₎	0.3 ₍₃₎	39.4 ₍₃₎	-	99.0

The standard deviation of the last digit is shown in parentheses. For olivine, the compositions are given that differ as much as possible from the initial one.

Results of relatively high-temperature experiments (1450 $^{\circ}\text{C}$). It has been experimentally established that at a sulfur concentration of 0.1

mol%, a polycrystalline olivine aggregate is formed, with single crystals of newly formed Ni-pyrrhotite and a sufficiently large amount of newly formed

orthopyroxene, as shown in Fig.1d. At 2 mol% sulfur, the formation of an association of recrystallized olivine with inclusions of sulfides, orthopyroxene and sulfide melt was established (Fig.1e). In contrast to relatively low-temperature experiments, olivine crystals are not characterized by a zonal structure; however, they demonstrate a sharp decrease in the FeO concentration to 3 wt% (Fig.2, Table 1). At the highest sulfur concentrations, the formation of an association of recrystallized olivine - practically iron-free, nickel-free, as well as newly formed orthopyroxene and sulfur-sulfide melt - was established (Fig.1f, Table 1).

As a result of the reconstruction of olivine sulfidation processes, it was found that at a relatively high temperature (1450 °C) occur: (1) recrystallization of olivine in a sulfur melt; (2) complete extraction of Fe and Ni from olivine into

sulfur melt; (3) the formation of sulfide or sulfur-sulfide melts; (4) formation of sulfide melt inclusions in olivine; (5) crystallization of newly formed orthopyroxene; (6) a decrease in the Fe and Ni contents in olivine to 0.

Conclusions. It was experimentally established that at a temperature of 1050 °C, an increase in the sulfur concentration in the system leads to the formation of zonal olivine crystals with an iron center and a magnesian periphery, a natural decrease in the iron content of olivine (in rims), and an increase in the amount and size of newly formed sulfides. At a relatively high temperature (1450 °C), an increase in the sulfur concentration in the system leads to a sharp decrease in the FeO and NiO contents in olivine, an increase in the amount of newly formed sulfide melt, while the formation of zonal crystals is not observed.

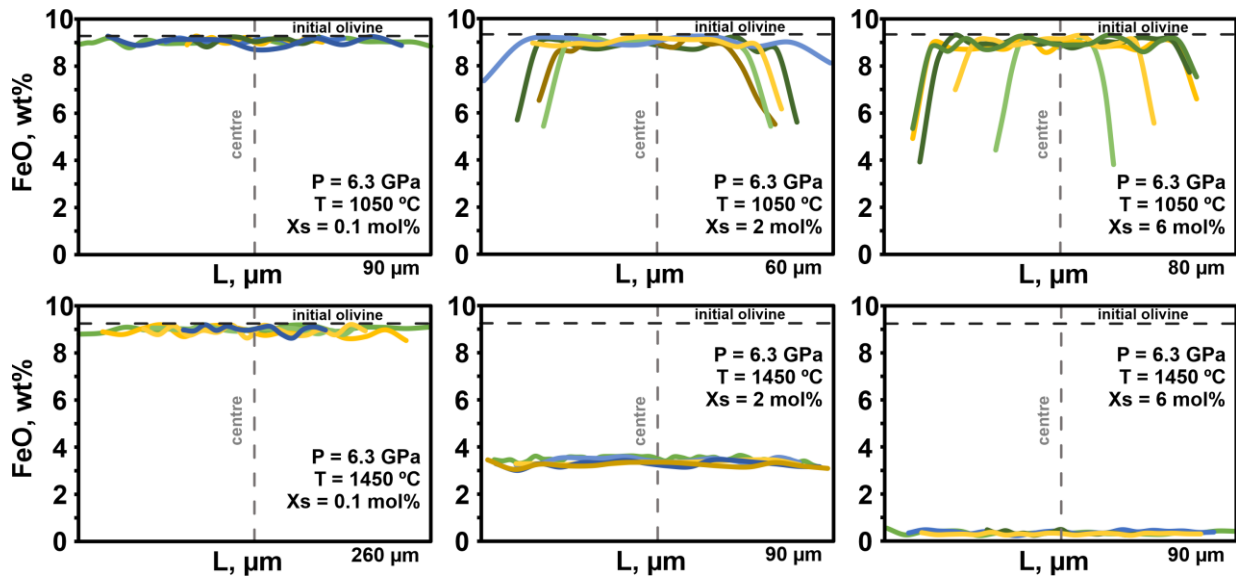


Fig.2. Profiles of compositions of olivine after experiments, depending on the concentration of sulfur

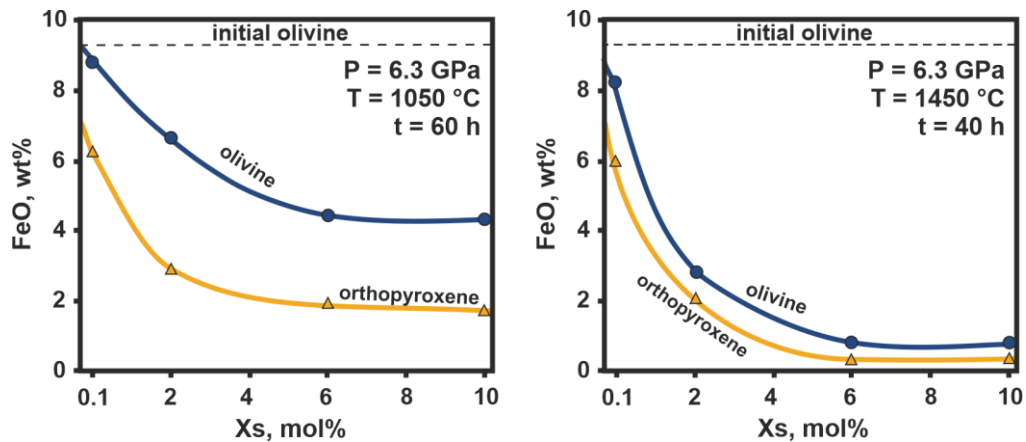


Fig.3. Graphs of the dependence of the compositions of the mineral phases obtained in the olivine - sulfur system on the sulfur concentration in the system (Xs). The compositions of olivines obtained in experiments with a sulfur concentration of 10 mol% are taken from Bataleva et al. (2016).

The established basic regularities are shown graphically in the diagrams in Fig.3. Both the increase in the sulfur concentration and the temperature of the experiments significantly increase

the intensity of olivine sulfidation. Summarizing the data obtained concerning the processes of sulfidation of ultrabasic rocks in nature, we can say that reducing agents of sulfur metasomatism, even in minimal concentrations, are capable of dissolving and transporting mantle silicates and sulfides, and play one of the key roles in ore-forming processes with the participation of mantle sulfur fluids.

Work is done on state assignment of the IGM SB RAS.

References

- Bataleva Yu.V., Palyanov Yu.N., Borzdov Yu.M., Sobolev N.V. (2016) Sulfidation of silicate mantle by reduced S-bearing metasomatic fluids and melts. *Geology*, 44 (4), 271-274.
- Evans K. A. (2012) The redox budget of subduction zones. *Earth-Science Reviews*, 113, 11-32.
- Fleet M.E., MacRae N.D. (1987) Sulfidation of Mg-rich olivine and the stability of niningerite in enstatite chondrites. *Geochimica et Cosmochimica Acta*, 51, 1511-1521.
- Kullerud G., Yoder H.S., Jr. (1963) Sulfide-silicate relations. Carnegie Institution of Washington Year Book, 62, 215-218.
- O'Reilly S.Y., Griffin W.L. (2013) Mantle metasomatism. in DE Harlov & H Austrheim (eds), *Metasomatism and the chemical transformation of rock: the role of fluids in terrestrial and extraterrestrial processes*. Lecture notes in earth system sciences. Springer, Springer Nature, 471-533.
- Papike J.J., Spilde M.N., Fowler G.W., Layne G.D., Shearer C.K. (1995) The Lodran primitive achondrite: Petrogenetic insights from electron and ion microprobe analysis of olivine and orthopyroxene. *Geochimica et Cosmochimica Acta*, 59, 3061-3070.
- Tomkins A., Evans K. (2015) Separate zones of sulfate and sulfide release from subducted mafic oceanic crust. *Earth and Planetary Science Letters*, 428, 73-83

Gorbachev N.S., Kostyuk A.V., Gorbachev P.N., Nekrasov A.N., Sultanov D.M. Phase relations and distribution of elements in the Fe-S-C system. UDC 552.11:553.21:550.89:552.351.2

Institute of Experimental Mineralogy RAS (gor@iem.ac.ru, nastya@iem.ac.ru)

Abstract. The phase relationships and distribution of siderophilic elements (SE) in the Fe-S-C system with an excess of carbon at P=4.0 GPa, T=1400°C were studied. The silicate melt contains inclusions of Fe-metal-sulfide melt with signs of immiscibility between Fe-C (Fm) and Fe-S (Fs) melts. Fm melt content Fe-Ni inclusions enriched with SE in the Pt - Os - Re sequence. Fractionation of Pt-Os-Re during the formation of inclusions in the Fe-S-C system can change the $^{190}\text{Pt} \rightarrow ^{186}\text{Os}$ and $^{187}\text{Re} \rightarrow ^{187}\text{Os}$ isotopic systems.

Keywords: melt, silicate, experiment, sulfide, differentiation, mantle.

Intruduction Equilibria of simple or binary Fe-containing melts with silicate melts are important for

understanding the problems associated with the processes of early differentiation of cosmic bodies at the stage of the magmatic ocean (MO). The separation of the Silicate melt Fe-metal melt (Fm) is associated with the differentiation of the MO, which served as the beginning of the early differentiation of cosmic bodies to form the Fe-Ni nucleus and silicate mantle. However, it turned out that during the separation of the metal component, for example, in the formation of the Earth's core, the content of strong siderophilic elements (HSE) in the earth's mantle is significantly higher than it should be based on the experimental coefficients of the HSE separation between metallic and silicate melts (Ringwood, 1996; Haine, 1995; Li, Agee, 1996, 2001). There are various hypotheses explaining this paradox: the late chondrite shell model (O'Neil, Palme, 1998), the model of "ineffective core formation" with an incomplete swelling of the metal phase (Jones, Drake, 1986), periodic seizure of the substance of the external kernel of superlumps and its mixing with a mantle material (Snow, Schmidt, 1998).

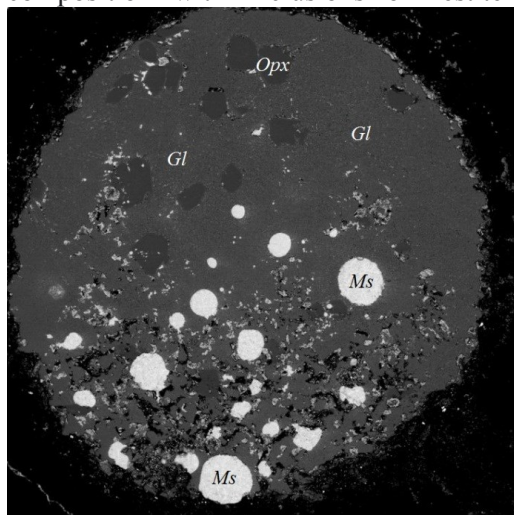
As a model of the Fe-metal component in the process of MO differentiation, the ternary Fe-S-C system is of greater interest. In this system, there is an immiscibility region between Fe-C and Fe-S melts (Wang et al., 1991). Taking into account the different ferrophilicity and chalcophilicity of HSE, we can expect their fractionation as a result of redistribution between metallic, sulfide and silicate melts, which can affect the compositions of coexisting phases. Although in a number of experimental studies, the immiscibility of Fe-C metallic and Fe-sulfide melts has already been used in the study of the processes of accretion, early differentiation of planets and their satellites (Gorbachev, Osadchy, 1980; Gorbachev et al., 1980; Gorbachev, 1990, Marakushev et al., 1995; Dasgupta et al., 2009; Hayden et al., 2011; Buono et al., 2011), however, the phase relations in the Fe-S-C-silicate system and distribution of HSE elements are still insufficiently studied. Some features of the phase relations in the peridotite-basalt-Fe-S-C system at the upper mantle P-T at 4 GPa, 1400°C are considered below

The method of the experiment The experiments were carried out at the IEM RAS on the "anvil with hole" NL-40 installation using a multi-ampoule quenching method. The initial sample consisted of fine powders of silicate (Gr peridotite, amphibolite) and Fe-bearing (a mixture of pyrrhotite, metallic Fe and carbon in the form of soot reagent) components, which were loaded into a graphite ampoule in layers, in the sequence peridotite-amphibolite-peridotite-FeS-Fe-C mixture. To clarify the behavior of HSE elements, Re, Os, Pt were added to the suspension – the most important metals of the metal-sulfide

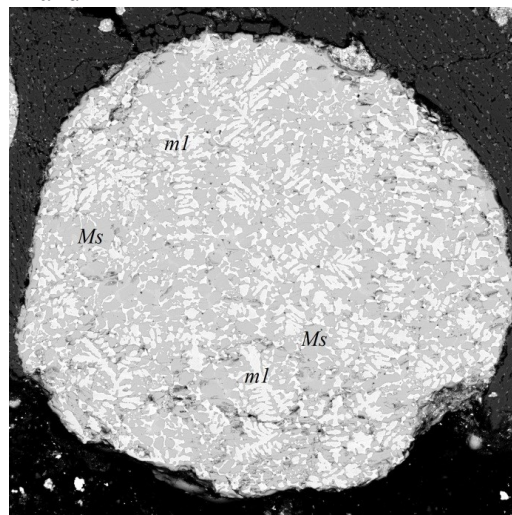
components of chondrites, Fe meteorites and magmatic sulfide ores. The graphite ampoule was placed in a Pt ampoule, which was hermetically brewed. The temperature is measured by a Pt₃₀Rh/P₁₆/Rh thermocouple. At high temperature, pressure is calibrated using a curve of the quartz-coesite equilibrium. Uncertainties are ± 10°C for temperature and ± 0.1 GPa for pressure measurement (Litvin, 1991). Duration of experiments was 6 hours. Products of experiments were studied by scanning electron microscope Tescan VEGA TS 5130MM with detector of secondary and backscattered electron on the YAG-crystals and energy dispersive X-ray microanalyzer with semi-conductor Si(Li) detector INCA Energy 350.

Results The matrix of the quenched sample consists of a silicate glass Gl of picrite-basalt composition with inclusions of restite Opx and

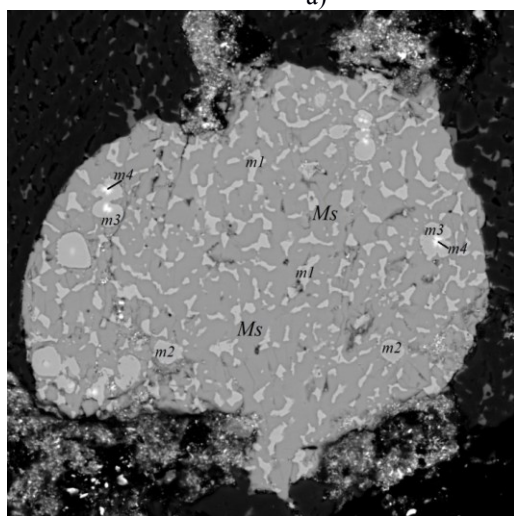
sulfide globules Ms with a diameter of up to 100 microns. According to the structure of the Fe-metal phase (m), two types of sulfide globules are distinguished: 1-with a Fe-sulfide matrix with inclusions enriched with Fe phase m1 of isometric form; 2-with a Fe-sulfide matrix with inclusions of Fe-metal phases in the different form: m1 - isometric form, quenching type + m2-in the form of globules without inclusions + m3-globules with refractory inclusions m4 Fe-Ni-Re-Os-Pt composition (Fig. 1). The criterion for the immiscibility of melts was the structure of quenching samples – sulfide globules in the glass of silicate matrices – immiscibility of sulfide and silicate melts, teardrop-shaped separation of the Fe-metal phase in an oval - shaped Fe-sulfide matrix-immiscibility of Fe-metal and Fe-sulfide melts.



a)



b)



c)

Fig.1. Micrographs of the quenched sample: a) silicate glass Gl picrite of basalt composition with inclusions of restite Opx, sulfide globules Ms; b) sulfide globule ms with inclusions of metal phases of the type of quenching decay structures m1; c) sulfide globule with inclusions of metal phases m1 type; m2 - metal globule without inclusions, m3 - metal globule with refractory inclusions Fe-Ni-Re-Os-Pt composition m4.

Representative compositions, in terms of 100 at.% of co-existing phases: Fe is a sulfide melt [matrix] Fe = 46.0 Ni = 3.5, Cu = 0.8, S = 49.7; Fe is

a metal melt, a globule in a sulfide matrix without inclusion of Fe = 84.5, Ni = 15.0, S = 0.5. Fe is a metal melt with inclusions of Fe = 85.5, Ni = 14.0, S

= 0.5; inclusion of the composition: Fe = 76.0, Ni = 11.1, Re = 10.9, Pt = 0.6, Os = 1.4 (Fig. 2).

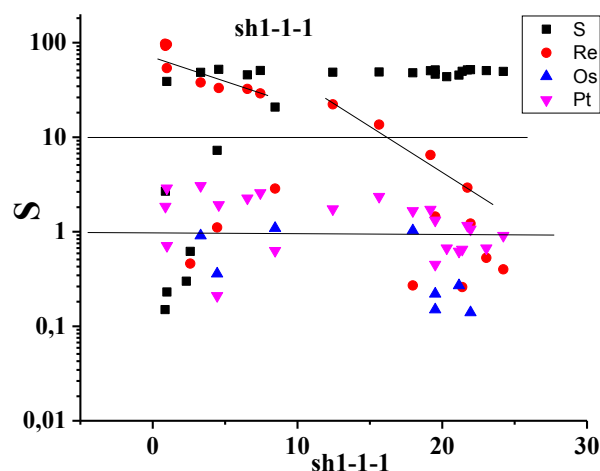


Fig. 2. Distribution of siderophilic elements in coexisting metal and sulfide phases. Lines show concentrations Re, Os, Pt in inclusions.

Discussion. The formation of refractory inclusions during saturation of the metal melt was accompanied by the fractionation of HSE elements, with the enrichment of Re inclusions relative to Os and Pt, and Pt – relative to Os with the separation coefficients of Fe and Ni between the metal melt and the inclusion of Fe ~2, Ni ~ 3 and the ratios in the inclusions of Re/Os~7.8, Pt/Os~0.43. These relations differ from the relations in chondrite and primitive mantle: chondrite-Re/Os=0.08, Pt/Os=2.06, PM-Re/Os=0.08, Pt/Os=2.09, which, despite the different concentrations in chondrite and PM according to McDonough, Sun, 1995, are similar. Thus, the formation of inclusions is accompanied by the fractionation of siderophilic elements with an increase in their concentrations in the sequence: Pt-Os-Re. Fractionation of Pt-Os-Re during the formation of inclusions in the Fe-S-C system can change the $^{190}\text{Pt} \rightarrow ^{186}\text{Os}$ and $^{187}\text{Re} \rightarrow ^{187}\text{Os}$ isotopic systems.

The work was performed in IEM RAS on the subject of NIR AAA-A18-118020590140-7

References

Buono A.S., R. Dasgupta, Cin-Ty A. Lee, D. Walker. Siderophile element partitioning between cohenite and liquid in the Fe–Ni–S–C system and implications for geochemistry of planetary cores and mantles // *Geochimica et Cosmochimica Acta*. 2013. 120, 239–250

Dasgupta R., A. Buono, G. Whelan, D. Walker. High-pressure melting relations in Fe–C–S systems: Implications for formation, evolution, and structure of metallic cores in planetary bodies // *Geochimica et Cosmochimica Acta*, 2009. V.73, P. 6678–6691

Gorbachev N.S. Early differentiation of meteorites and planets. *Lunar and Planetary Science*, Houston, Texas. 1980 XI. P. 181

Gorbachev N.S. Fluid-magma interaction in sulfide-silicate systems. *Internat. Geology Rev.*, 1990. V.32. N.8.P. 749-831

Gorbachev N.S., Osadchy E.G. It is not necessary in silicate melts as a factor in the early differentiation of meteorites and planets. *Dan USSR*. 1980. V. 255, №36 pp. 693-697.

Hain V.E. The main problems of modern geology (geology on the threshold of the XXI century). M. Science. 1995. S. 190.

Hayden L.A., James A. Van Orman, William F. McDonough, Richard D. Ash, Cyrena A. Goodrich. Trace element partitioning in the Fe–S–C system and its implications for planetary differentiation and the thermal history of ureilites // *Geochimica et Cosmochimica Acta*. 2011. 75, 6570–6583

8.Jones J. H., Drake M. J. Geochemical constraints on core formation in the Earth // *Nature*, 1986. V. 322, P. 221-228.

Marakushev A.A. Experimental study of chondrites education processes // *DAN*. 1995. T 345, №6, p. 797-801.

Li J., Agee C.B. Geochemistry of mantle–core differentiation at high pressure // *Nature*, 1996. V. 381, P. 686-689.

Li, J., Agee, C.B. Element partitioning constraints on the light element composition of the Earth's core // *Geophys. Res. Lett.* 2001. 28, 81–84.

Litvin Yu.A. Physico-chemical studies of melting of the deep substance of the Earth. M.: Science. 1991. 312 p.

McDonough W. F., Sun S. S. The composition of the Earth // *Chem. Geol.*, 120, 223-253, 1995.

O'Neil H. St. C., Palme H. Composition of silicate Earth: implications for accretion and core formation // *The Earth's Mantle: Composition, Structure and Evolution*. University Press, Cambridge. 1998. pp. 3-126.

Ringwood A. E. Composition of the core and implications for origin of the Earth // *Geochem. J.*, 1996, 11, 111-135.

Snow J. E., Schmidt G. Constraints on Earth accretion deduced from noble metals in oceanic mantle // *Nature*, 1998. V. 391, P. 166-169.

Wang C., Hiram J., Nagasaka T. and Ban-ya S. Phase equilibria of liquid Fe–S–C ternary system // *ISIJ Int.* 1991. 31, 1292–1299.

Iskrina A.V.^{1,2}, Bobrov A.V.^{1,2,3}, Spivak A.V.², Kuzmin A.V.⁴, Chariton S.⁵, Fedotenko T.⁶, Dubrovinsky L.S.⁷. Experimental study of postspinel phases in the system Ca–Al–O and Mg–Al–Cr–O at the conditions of the Earth's transition zone and lower mantle UDC 549.02

¹Lomonosov Moscow State University, Moscow, ²D.S. Korzhinskii Institute of Experimental Mineralogy RAS, Chernogolovka, ³Vernadsky Institute of Geochemistry and Analytical Chemistry RAS, Moscow, ⁴Institute of Solid State Physics RAS, Chernogolovka, ⁵Center for Advanced Radiations Sources, University of Chicago, Chicago, ⁶Material Physics and Technology at Extreme Conditions, Laboratory of Crystallography, Universität Bayreuth,

Germany, ⁷Bavarian Research Institute of Experimental Geochemistry and Geophysics (BGI) Bayreuth, Germany (iskrina@iem.ac.ru)

Abstract. Phases with the structures of calcium ferrite, calcium titanate, and marokite are considered as post-spinel phases and can concentrate various elements (for example, Al, Fe, Mg, Na, Cr, etc.) at the conditions of the transition zone and the lower mantle of the Earth. In the Ca-Al±Fe-O system, the compressibility of the Ca(Fe,Al)₂O₄ phase was studied up to 61 GPa, and the equation of state was obtained. No phase transition was detected, but a spin transition was registered. The Mg₂(Al,Cr)₂O₅ and Mg(Cr,Al)₂O₄ phases were formed in the Mg-Al-Cr-O system. The Mg(Al,Cr)₂O₄ phase was studied using *in situ* Raman spectroscopy up to 30 GPa. At 12-16 GPa the color of the sample changed from green to red. A gradual evolution in the Raman spectra was observed at high pressure. According to the data of Raman spectroscopy, it was revealed that the structure of Mg(Al,Cr)₂O₄ phase does not undergo serious changes up to 30 GPa.

The obtained data confirm the possibility of the existence studied phases at high pressures and suggest their active role as the concentrator phases of elements at deep shells.

Keywords: *phase relations; postspinel phases; transition zone; lower mantle; HP-HT experiment; spin transition; equation of state*

Spinel is a widespread mineral found in various geological environments. However, the region of its stability is limited, and at great depths there is a transformation into the so-called postspinel phases (Akaogi et al., 1999). Phases with structures of calcium ferrite (CF), calcium titanate (CT) and marokite are considered as the main candidates for the role of postspinel phases (Decker and Kasper, 1957, Rogge et al., 1998, Giesber et al., 2001).

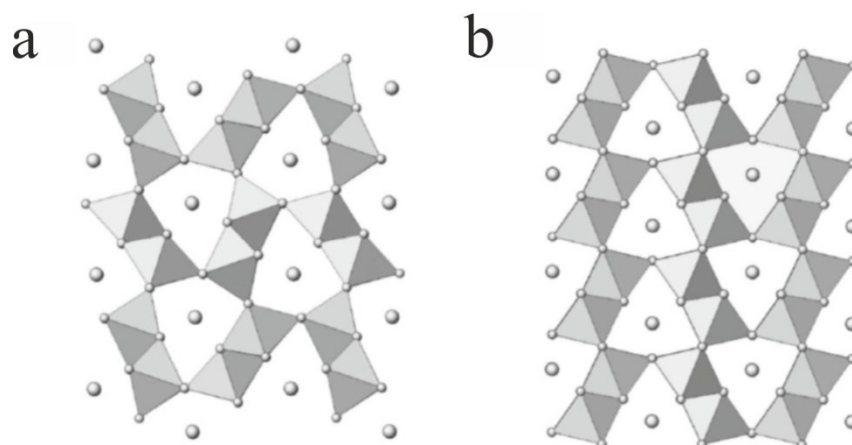


Fig. 1. Structures image: **a** – calcium ferrite *Pnma*; **b** – calcium titanate *Bbmm* (by Eremin et al., (2016)).

The structure of the postspinel phases is formed by edge and corner octahedra with channels parallel to the *b* axis (CF structure) and the *a* axis (CT structure), respectively. These two structures contain dodecahedral and octahedral positions. Within this family of topology-related structures with a "marokite" channel formed by six octahedra, structures with centered *Cmcm* (*Bbmm*) and with primitive *Pnma* (*Pmcm*), *Pbcm* (*Pmab*) cells are distinguished. In the first structure with a centered cell, the position of the A²⁺ cation in the tunnel is strictly straight (Fig. 1b), while in the second structure, the position A²⁺ is slightly "rotated" (to nearby tunnels) (Fig. 1a) (Eremin et al., 2016).

Structures with a "marokite" channel can include various cations, for instance, Cr, Al, Mg, Fe, Ca, Ti, Fe, Na, forming of solid solutions. This is the main reason that natural postspinel phases aren't homogeneous in composition (Kaminsky, 2017). To date, several end members of the series of solid solutions are known-NaAlSiO₄, MgAl₂O₄, CaCr₂O₄, FeCr₂O₄ (Liu, 1977; Irifune et al., 1991; Chen et al. 2008). In this work, the conditions of formation and

structural features of high-impact phases in the Ca-Al-O and Mg-Al-Cr-O systems were studied.

The experiments were carried out using a 1200-t multi-anvil Sumitomo press at the Bayerisches Geoinstitut (Bayreuth, Germany). The starting powders were homogenized in the agate mortar and then annealed in platinum crucibles for 24 hours at 1000°C. The ready starting mixture was placed into a capsule made of a 0.25 mm platinum foil. Experiments on multi-anvil press were carried out using standard 7/3 assemblages. Experiments on the synthesis of phases in the Ca-Al-O system with the addition of Fe were carried out at 24 GPa, T=1600°C, and in the Mg-Al-Cr-O system at pressures of 18 and 24 GPa and a temperature of 1600C with an exposure time from 1 to 5 hours. The phase composition was determined using a scanning electron microscope CamScanM2300 (VEGA TS 5130MM) with the Link INCA spectral analyzer in the IEM RAS. The accelerating voltage was 20 kV. The beam current was ~10nA. The average of compositions of the studied phases was determined by 8 analyses.

The structure of newly formed phases was determined by single-crystal X-ray diffraction using a Bruker SMART APEX CCD diffractometer with Rigaku rotating anode (Rotor Flex FR-D, Mo-K α radiation) and Osmic focusing X-ray optics at the Bayerisches Geoinstitut, Germany and Rigaku Oxford Diffraction "Gemini R" CCD diffractometer with graphite monochromated MoK α radiation ($\lambda=0.71073$ Å) at the Institute of Solid State Physics RAS.

Raman spectra of experimental samples were obtained using an Acton SpectraPro-2500i spectrograph with a CCD Pixis2K cooling detector up to -70C and an Olympus microscope with a 532 nm monomeric laser at Institute of Experimental Mineralogy RAS.

Electronic structure calculations of $S = 1/2$, $3/2$ and $5/2$ spin states of the Fe(III) aqua clusters was performed at DFT level theory employing the spin-unrestricted B3LYP (Becke, 1988) hybrid functional and ORCA software (Neese, 2012).

In the Ca-Al-O(+Fe) system, the Ca(Fe,Al) $_2$ O $_4$ phase was synthesized in experiments at a pressure of 24 GPa. By single-crystal X-ray diffraction was determined that the studied phase has a calcium ferrite structure and a $Pnma$ space group.

The compressibility of the Ca(Fe,Al) $_2$ O $_4$ phase was studied using a synchrotron radiation source at ESRF (Grenoble) up to ~61 GPa. No phase transformations were detected in this pressure range, but a spin transition for iron was registered. It was also possible to obtain the equation of state for the Ca(Fe,Al) $_2$ O $_4$ phase (Fig. 2).

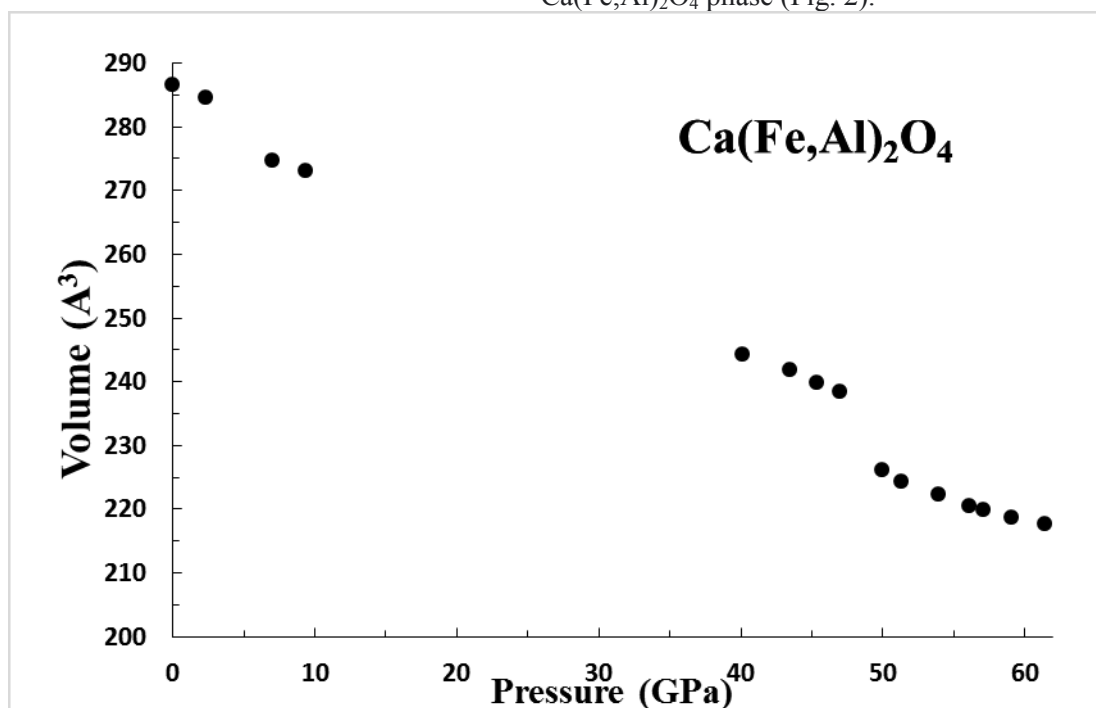


Fig. 2. Equation of state for Ca(Fe,Al) $_2$ O $_4$ phase.

The stability of different spin states of the iron(III) atom within distorted FeO $_6$ octahedra at low and high pressure was analyzed by the quantum chemistry methods. In order to simplify calculations, the new aqua complexes [Fe(H $_2$ O) $_6$] $^{3+}$ were constructed based in FeO $_6$ octahedra at 2.3 GPa and 53.9 GPa pressures. The main difference between [Fe(H $_2$ O) $_6$] $^{3+}$ octahedra at low and high pressures consists in the relative change in energy (ΔE) for the different spin states: $S=5/2$ state of Fe(III) complex is the most favorable state at low pressures while the lowest $S=1/2$ spin state is more stable at high pressures. This confirms the change in the spin state of Fe (III) in the studied pressure range.

In experiments at pressures of 18 and 24 GPa, the Mg $_2$ (Al,Cr) $_2$ O $_5$ and Mg(Cr,Al) $_2$ O $_4$ phases were synthesized. They are green crystals ranging in size

from 30 to 60 μ m. Single crystals were selected for further research.

The Mg $_2$ (Al,Cr) $_2$ O $_5$ phase has a modified ludwigite (mLd) structure ($Pbam$ space group), which was also observed for Mg $_2$ Al $_2$ O $_5$ and Fe $_2$ Cr $_2$ O $_5$ compounds (Enomoto et al., 2009). It is possible that this structure is "intermediate", excluding the possibility of a direct transition from a calcium ferrite to a calcium titanate structure in a certain pressure range. However, this assumption requires further clarification.

The Mg(Cr,Al) $_2$ O $_4$ phase has a calcium titanate structure and crystallizes in the $Cmcm$ space group. It was studied up to 30 GPa in a diamond anvil cell (DAC). As a result, it was found that when the crystal reaches 12-16 GPa, the color of the crystal changes from green to red, which persists even with a

further increase in pressure. This change is not stable, and when the pressure decreases, the crystal turns green again. This effect is associated with the contribution of the trigonal component to the octahedral coordination of $(\text{Cr,Al})\text{O}_6$, as a result of which the parameter $-3/2K$ changes. Below a pressure of 6 GPa, compression is mostly isotropic, but above this value, the trigonal distortion increases rapidly with pressure (Sugano et al., 1958).

Based on the results of this study, it can be concluded that in the Ca-Al-O system, the $\text{Ca}(\text{Fe,Al})_2\text{O}_4$ phase is stable in a wide range of pressures and temperatures up to lower mantle; and is one of the end members of a number of solid solutions of post-spinel phases crystallizing in the structural type CF; at the same time, in the Mg-Al-Cr-O system, the presence of a phase with the structure CT and a phase with the structure mLd is observed. The above-described phases are undoubtedly stable under mantle conditions, can be considered as postspinel phases and as concentrators of aluminum and other elements in the deep layers of the Earth.

This study was supported by the Russian Foundation for Basic Research, project №20-35-90095\20. This study carried out within the scientific plan of the Laboratory of deep geospheres of the Lomonosov Moscow state University and within the Research Program of the D.S. Korzhinskii Institute of Experimental Mineralogy Russian Academy of Sciences (AAAA-A18-118020590140-7).

References

- Akaogi M., Hamada Y., Suzuki T., Kobayashi M. and Okada M. (1999) High pressure transitions in the system MgAl_2O_4 - CaAl_2O_4 : A new hexagonal aluminous phase with implication for the lower mantle. *Phys. Earth Planet. Inter.* 115, 67–77.
- Becke A.D. Density-functional exchange-energy approximation with correct asymptotic behavior // *Phys Rev A.* 1988. Vol. 38, № 6. P. 3098–3100.
- Chen M., Shu J. F. and Mao H. K. (2008) Xieite, a new mineral of high-pressure FeCr_2O_4 polymorph. *Chinese Sci. Bull.* 53, 3341–3345.
- Decker B. F. and Kasper J. S. (1957) The structure of calcium ferrite. *Acta Crystallogr.* 10, 332–337.
- Enomoto, A., Kojitani, H., Akaogi, M., and Yusa, H. High-pressure transitions in MgAl_2O_4 and a new high-pressure phase of $\text{Mg}_2\text{Al}_2\text{O}_5$. *Journal of Solid State Chemistry*, 182. 2009. P. 389–395
- Eremin N. N., Grechanovsky A. E., Marchenko E. I. Atomistic and ab initio modeling of CaAl_2O_4 high-pressure polymorphs under Earth's mantle conditions// *Crystallography Reports.* 2016. 61(3). P. 432–442.
- Giesber H. G., Pennington W. T. and Kolis J. W. (2001) Redetermination of CaMn_2O_4 . *Acta Crystallogr. Sect. C Cryst. Struct. Commun.* 57, 329–330.

- Irifune, T., Fujino, K., & Ohtani, E. A new high-pressure form of MgAl_2O_4 // *Nature.* 1991. 349 (6308), P. 409–411.
- Kaminsky F.V. *The Earth's Lower Mantle: Composition and Structure*// Springer Geology. 2017. P. 340.
- Liu L. High pressure NaAlSiO_4 : The first silicate calcium ferrite isotype// *Geophysical Research Letters.* 1977. 4(5). P. 183–186.
- Neese F. The ORCA program system // *Wiley Interdiscip Rev Comput Mol Sci.* 2012. Vol. 2, № 1. P. 73–78.
- Rogge M. P., Caldwell J. H., Ingram D. R., Green C. E., Geselbracht M. J. and Siegrist T. (1998) A New Synthetic Route to Pseudo-Brookite-Type CaTi_2O_4 . *J. Solid State Chem.* 141, 338–342.
- Sugano S., Tanabe Y., Tsujikawa I. (1958) Absorption spectra of Cr^{3+} in Al_2O_3 . *J. Phys. Soc. Japan*, 13, 880–899.

Kostyuk A.V., Gorbachev N.S., Nekrasov A.N., Sultantov D.M. Melting of garnet-bearing carbonatite at the parameters of the upper mantle (T=950-1400°C, P=4 GPa) UDC 550.4.02

IEM RAS, Chernogolovka, Moscow district (nastya@iem.ac.ru, gor@iem.ac.ru)

Abstract. Melting of garnet-bearing carbonatite from the Tromsø Nappe, Norway has been experimentally studied in a «dry» and $\text{H}_2\text{O}+\text{CO}_2$ -containing system at $T = 950$ – 1400°C , $P = 4.0$ GPa. The experiments were carried out on an anvil-with-hole apparatus using a multi-ampoule quenching technique at the IEM RAS. The melting of the carbonatite at $T = 950$ – 1400°C , $P = 4.0$ GPa showed that the “dry” solidus temperature is 1150°C , and the liquidus temperature is $>1300^\circ\text{C}$. In the experiment with $\text{H}_2\text{O} + \text{CO}_2$ fluid, the solidus and liquidus temperatures are $\leq 950^\circ\text{C}$ and 1250°C , respectively. The subsolidus association is calcite, garnet, clinopyroxene, biotite, and accessory minerals: apatite, ilmenite, rutile, and titanite. The garnet and carbonatite melt occur in reaction relationships, as is evident from the garnet zoning with a decrease in the FeO and increase in the MgO, CaO, TiO_2 , and LREE concentrations. Experimental data indicate that the garnet-bearing carbonatites in the Tromsø area were formed in relation to the carbonatization and melting of upper mantle material at high pressures with subsequent intrusion and crystallization of silicate-carbonate magmas.

Keywords: garnet-bearing carbonatite, experiment, high T–P conditions, melting, upper mantle

Introduction. For the characterization of primary mantle carbonatites and their genesis, carbonatites containing inclusions of high-pressure minerals are of great interest. These include garnet-bearing carbonatites from the Tromsø region, Norway (Ravna et al., 2006, 2017; Janák et al., 2012). The rocks were affected by ultrahigh-pressure metamorphism to the diamond depth facies during the collision of the Baltica and Laurentia plates in the course of the Caledonian orogeny (Janák et al., 2013, 2012; Ravna and Roux, 2006). To determine the physicochemical conditions under which the garnet-

bearing carbonatite was produced, we studied its anhydrous melting at $T = 950\text{--}1400^\circ\text{C}$ and $P = 4.0$ GPa and its melting in the presence of $\text{H}_2\text{O} + \text{CO}_2$ fluid at the same $P\text{--}T$ parameters.

Experimental and analytical methods. The experiments were carried out at the IEM RAS on an anvil-with-hole apparatus (NL-40) using a multi-ampoule technique with Au, Au–Pd, and Pt capsules (Gorbachev, 1990). The starting materials were finely powdered garnet-bearing carbonatite from Tromsø, and the source of $\text{H}_2\text{O} + \text{CO}_2$ (15 wt %) was oxalic acid dihydrate $\text{H}_2\text{C}_2\text{O}_4 \cdot 2\text{H}_2\text{O}$. The temperature was measured with a $\text{Pt}_{30}\text{Rh}/\text{Pt}_6/\text{Rh}$ thermocouple, and the pressure at high temperatures was calibrated on the quartz–coesite equilibrium curve. The temperature and pressure were measured accurate to $\pm 10^\circ\text{C}$ and ± 1 kbar, respectively (Litvin, 1991). The experimental runs lasted for 8–16 h. Polished samples of the experimental products were studied and analyzed on a VEGA TS 5130MM PC-controlled scanning electron microscope equipped with YAG-based detectors of secondary and back-

scattered electrons and with an energy dispersive X-ray microprobe with an INCA Energy 350 Si(Li) detector.

Results. Anhydrous carbonatite melting. The experiments on anhydrous carbonatite melting were conducted at $950\text{--}1300^\circ\text{C}$ and 4 GPa. The anhydrous solidus temperature was close to 1150°C . The subsolidus assemblage at 950 and 1050°C consisted of carbonate, garnet, clinopyroxene, biotite, and accessory apatite, ilmenite, and titanite. The carbonate was calcite with approximately 5–6 wt % $\text{FeO} + \text{MgO}$ and with low concentrations of SiO_2 , Al_2O_3 , TiO_2 , Na_2O , and K_2O . The garnet was found as large (50–100 μm) anhedral (partly melted) grains of the composition $\text{pyr}_{10}\text{--gros}_{30}\text{--alm}_{60}$. The clinopyroxene developed as tabular grains of diopside–hedenbergite composition, $(\text{Ca}_{0.7}\text{Mg}_{0.5}\text{Fe}_{0.3})(\text{Al}_{0.1}\text{Na}_{0.1})\text{Si}_2\text{O}_6$. The clinopyroxene grains ranged from 20 (at 950°C) to 100 μm (at 1050°C) (Figs. 1a, 1b).

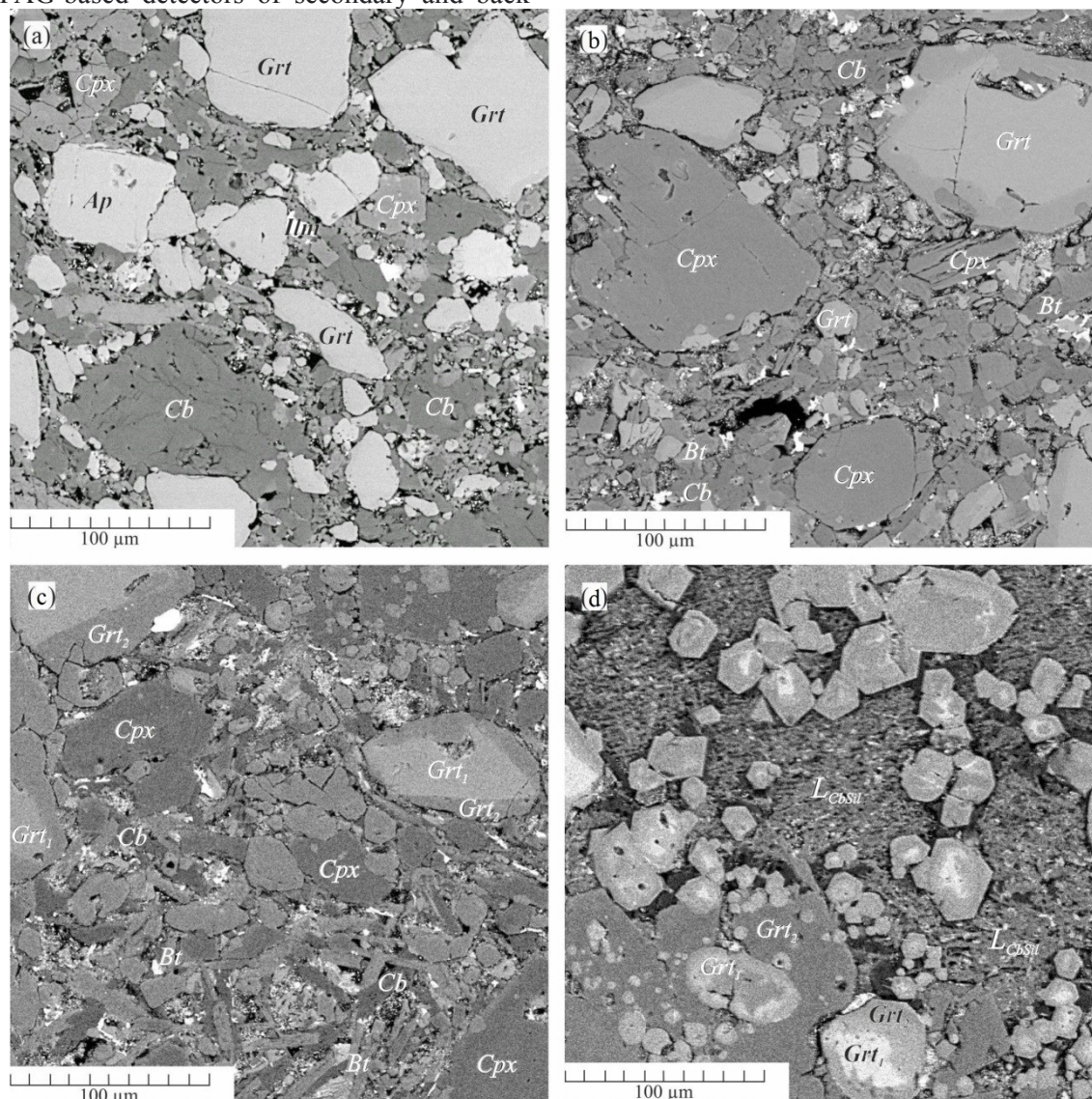


Fig. 1. BSE images of quenched samples after anhydrous carbonatite melting at (a) 950°C , (b) 1050°C , (c) 1150°C , (d) 1300°C .

The supersolidus association at 1150°C consisted of quenched carbonatite melt, calcite, garnet, clinopyroxene, biotite, and accessory apatite, ilmenite, and rutile (Fig. 1c). The large (up to 100 μm) grains of clinopyroxene (Ca_{0.8}Mg_{0.5}Fe_{0.3})(Al_{1.0}Na_{0.1})Si₂O₆ and equally large garnet grains were hosted in a carbonate matrix (*L_{Cb}*) with numerous small grains of accessory minerals and silicate phases (*Bt*, *Cpx*, *Ap*, and *Ilm*). The fact that the carbonate matrix contains notable concentrations of major oxides (more than 7 wt % FeO + MgO and up to 5% SiO₂ + Al₂O₃ + TiO₂ + Na₂O + K₂O) provides evidence of carbonatite melt. The garnet was zoned: the core had a composition identical to that of the subsolidus garnet, *pyr*₁₀–*gros*₃₀–*alm*₆₀, and the margins were richer in TiO₂, CaO, and MgO and had the composition *pyr*₂₀–*gros*₄₀–*alm*₄₀.

At 1300°C, the zoned garnet coexisted with the carbonatite matrix. Figure 1d displays a clearly seen garnet core (*Grt-1*), FeO-enriched parts of the

composition *pyr*₁₅–*gros*₃₀–*alm*₅₅, and marginal parts (*Grt-2*) of reaction garnet, which are enriched in MgO and CaO and have the composition *pyr*₂₅–*gros*₅₀–*alm*₂₅. When quenched, the carbonatite melt produced a mixture of microlites of variable composition, from carbonate–silicate to silicate–carbonate.

Melting of Carbonatite in the Presence of H₂O + CO₂ Fluid. When garnet-bearing carbonatite was melted in the presence of H₂O + CO₂ fluid, the solidus temperature was $T \leq 950^\circ\text{C}$. The carbonatite melt coexisted with calcite, garnet, clinopyroxene, apatite, and biotite. The sample was poorly cemented. Some large (up to 100 μm) garnet grains of the composition *pyr*₁₀–*gros*₃₀–*alm*₆₀ were surrounded by aggregates of small needles, crystals, and poorly preserved grains of *Cpx*, *Bt*, *Cal*, and *Ap* (Fig. 2a).

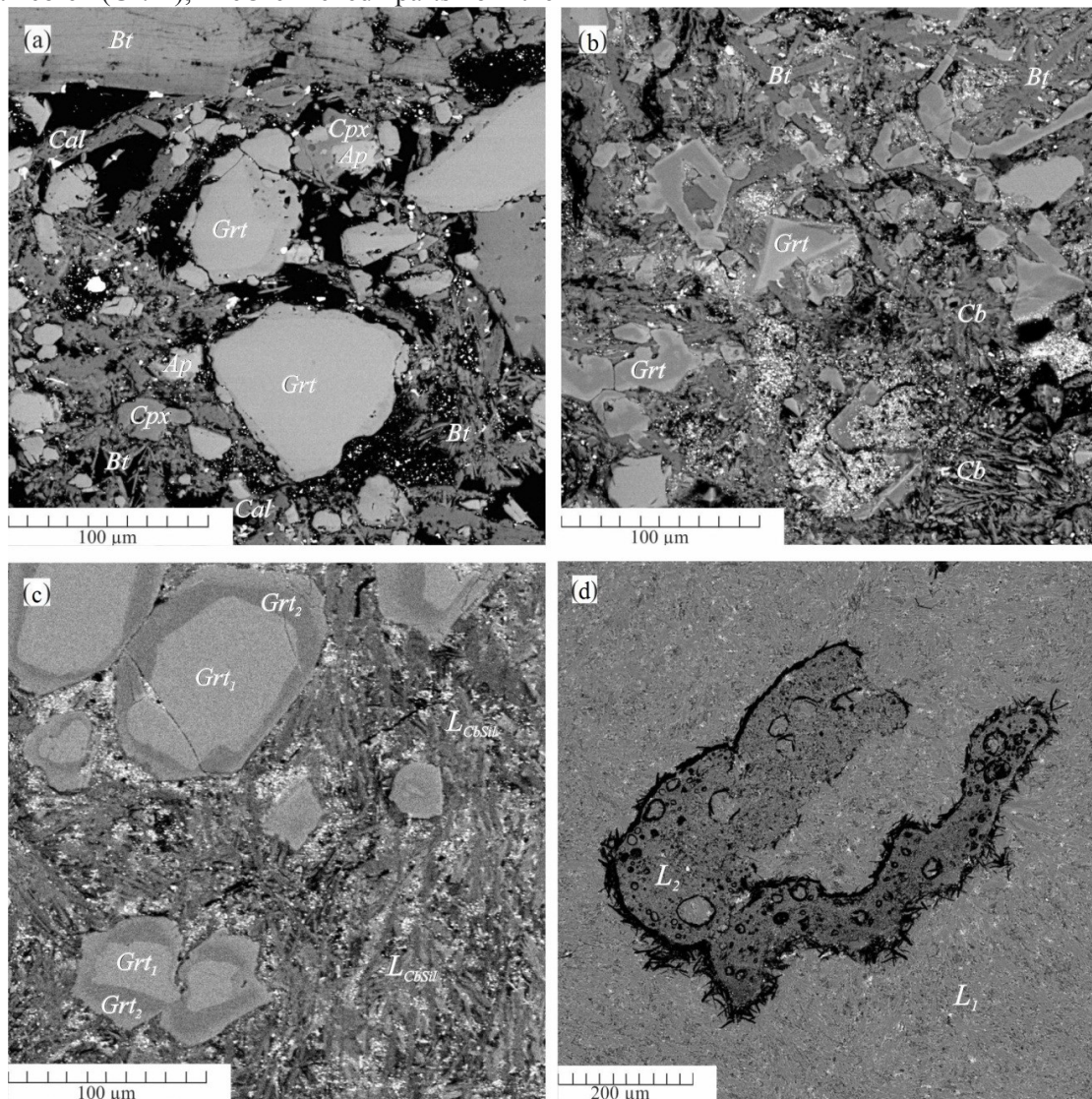


Fig. 2. BSE images of quenched samples after carbonatite melting in the presence of H₂O + CO₂ fluid at (a) 950°C, (b) 1050°C, (c) 1150°C, (d) 1400°C.

A temperature increase to 1050°C was associated with an increase in the proportion of carbonatite melt, and the products contained calcite, garnet, and biotite but no clinopyroxene (Fig. 2b). The quenched carbonatite melt (mixture of carbonate microlites) filled the space between fragments of garnet grains (*pyr*₁₅–*gros*₅₀–*alm*₃₅) and long columnar biotite crystals.

At temperatures of 1150–1250°C, the carbonatite melt (*L_{CbSil}*) coexisted with zoned garnet, whose reaction rims (*Grt-2*) are poorer than the garnet cores (*Grt-1*) in FeO and MnO and richer in MgO, CaO, and TiO₂ (Fig. 2c). The liquidus temperature was 1250°C.

A temperature increase led to the dissolution of the silicate phases, which saturate the carbonatite melt. In the underliquidus (at *T* ≥ 1300°C), the sample consists of a carbonate–silicate matrix, which exsolved into immiscible carbonate and silicate

liquids (*L*₁ and *L*₂) with the crystallization of graphite at 1400°C (Fig. 2d). The chemical compositions of *L*₁ and *L*₂ recalculated to 100 wt % are only insignificantly different. The differences in the concentrations of major oxides do not exceed 1–2 wt %.

Comparative analysis of the chemical composition of the garnet before and after the experiments shows that the cores of the experimental garnet (*Grt-1*) correspond to the relict garnet (*Grt₁*) of the Tromsø carbonatite (tabl.1). The CaO, FeO, MgO, and TiO₂ concentrations are identical, in contrast to the marginal reaction zone. CaO and FeO concentrations in the reaction rims of the experimental garnet (*Grt-2*) and the second-generation garnet (*Grt₂*) are similar, and the MgO and TiO₂ concentrations are one order of magnitude lower in the experimental samples.

Tabl. 1. Chemical composition of garnet in carbonatite Tromsø and in experiment sample (1150°C, 4 GPa)

	SiO ₂	TiO ₂	Al ₂ O ₃	FeO	MnO	MgO	CaO	Na ₂ O	K ₂ O	P ₂ O ₅	Cr ₂ O ₃	Cymma
Garnet in carbonatite												
<i>Grt₁</i>	37.77	0.13	21.00	23.00	0.32	5.92	10.67	0.22	< π/o	< π/o	< π/o	99.03
<i>Grt₂</i>	36.30	0.18	23.09	9.31	0.07	0.82	18.78	0.11	< π/o	0.09	0.07	89.45
Experimental garnet in “dry” system												
<i>Grt-1</i>	36.88	0.19	20.08	24.53	0.89	4.15	10.76	0.08	0.01	0.07	0.00	97.63
<i>Grt-2</i>	37.91	1.00	21.03	14.80	0.42	6.50	16.09	0.04	0.02	0.03	0.16	97.98
Experimental garnet in system with H ₂ O+CO ₂ fluid												
<i>Grt-1</i>	37.16	1.52	19.49	20.41	0.76	4.92	13.50	0.09	0.05	0.16	0.06	97.91
<i>Grt-2</i>	37.16	3.27	19.49	12.43	0.49	6.80	18.46	0.16	0.08	0.75	0.09	97.46

Note: *Grt₁*– relicts garnet, *Grt₂* – second generation of garnet in carbonatites; *Grt-1* – core, *Grt-2* – rim of experimental garnet.

Conclusions. The melting of the garnet-bearing carbonatite has demonstrated that the anhydrous solidus temperature is 1150°C, and the liquidus temperature is >1300°C. The subsolidus mineral assemblage at 950–1150°C consists of calcite, garnet, clinopyroxene, biotite, and accessory minerals. The zoning of the garnet indicates that it interacted with the carbonatite melt. In the anhydrous system, the association carbonatite melt–garnet, which is typical of the naturally occurring carbonatite, was formed within the temperature range of 1150–1300°C. In the experiments with H₂O + CO₂ fluid, the solidus temperature was ≤950°C, and the liquidus temperature was ≥1250°C. The association of carbonatite melt with garnet, which is typical of the Tromsø carbonatite, was produced within the temperature range of 950–1250°C.

Our results show that the zoned garnet of the experimental samples is similar in composition to the garnet of first through third generations in the natural carbonatite. The cores of the experimental garnet grains are relicts of the natural garnet (*Grt₁*), and their

marginal parts are characterized by higher MgO and TiO₂ concentrations than in the naturally occurring second-generation reaction garnet (*Grt₂*). No such efficient LREE enrichment in garnet was detected in the experiment.

References

- Litvin Yu.A. (1991) Physicochemical studies of the melting of deep-seated matter of the Earth. M.: Science. 312 s.
- Broska, I., Ravna, E. J. K., Vojtko, P., Janak, M., Konecny, P., Pentrak, M., Bacik, P., Luptakova, J. & Kullerud, K. (2014) Oriented inclusions in apatite in a post-UHP fluid-mediated regime (Tromsø Nappe, Norway) // *Europ J. Mineralogy*. 26, 623–634.
- Gorbachev N.S. (1990) Fluid-magma interaction in sulfide-silicate systems // *Intern Geol Review*. 32 (8), 749–831.
- Janák M., Ravna E.J.K., Kullerud K. (2012) Constraining peak P-T conditions in UHP eclogites: Calculated phase equilibria in kyanite- and phengite-bearing eclogite of the Tromsø Nappe, Norway // *J Metamorphic Geol*. 30, 377–396.

- Ravna E.J.K., Kullerud K., Ellingsen E. (2006) Prograde garnet-bearing ultramafic rocks from the Tromsø Nappe, northern Scandinavian Caledonides // *Lithos*. 92, 336–356.
- Ravna E.J.K., Roux M.R.M. (2006) Metamorphic evolution of the Tønsvika eclogite, Tromsø Nappe - Evidence for a new UHPM province in the Scandinavian Caledonides // *Intern Geol Review*. 48, 861–881.

Kuzyura A.V., Litvin Y.A. Peritectic reaction of olivine in the system olivine-jadeite-diopside-garnet ±(C-O-H) as a clue mechanism of ultrabasic to basic evolution of the upper mantle magmatism (experiment at 6.0 GPa). UDC 552.11

Korzinskii Institute of Experimental Mineralogy RAS
(shushkanova@iem.ac.ru, litvin@iem.ac.ru)

Abstract. Experimental researches at 6.0 GPa and 1200–1650°C of phase relations at melting of systems Ol-Jd-Di-Grt and Ol-Jd-Di-Grt-(C-O-H) were carried out with using of polythermal sections Ol-Omph and Ol₉₅(C-O-H)₅-Omph₉₅(C-O-H)₅. A peritectic reaction of olivine and a melt enriched in Jd-component with a formation of garnet was found out. Fractional magmatic evolution occurs at ultrabasic to basic compositions, it is controlled by a set: cotectic L+Ol+Cpx+Grt → peritectic Ol+Jd-L with a formation of a garnet Grt → cotectic L+Omph+Grt. Peritectic L+Ol+Cpx/Omph+Grt is like "a physico-chemical bridge" providing a transformation from ultrabasic magmas to basic ones, from peridotite/pyroxenite rocks to eclogite ones. C-O-H-fluids don't change phase relations of ultrabasic-basic system Ol-Jd-Di-Grt-(C-O-H), lowering solidus and liquidus temperature on 120 and ~60-80°C and raising a composition of the peritectic reaction concerning Mg- и Fe-components on ~10 wt. %.

Keywords: *eclogite; peridotite; fractional crystallization; ultrabasic to basic evolution; peritectic reaction; olivine garnetization; C-O-H-fluid.*

Mineralogical and petrological studies of xenoliths in kimberlites indicate physicochemically unified processes of formation of peridotite-pyroxenite-eclogite series of magmatic rocks of the garnet-peridotite facies of the upper mantle. Thus, petrochemical trends of increasing concentrations of Ca- and Fe- components in garnets, Fe and Na in clinopyroxenes and omphacites (Sobolev, 1974), Ca and Al - in coexisting garnets and clinopyroxenes of both olivine-normative garnet peridotites and garnets and omphacites of silica-normative eclogites (MacGregor, Carter, 1970), as well as Al and Fe - in peridotite and eclogite rocks (fig. 1) demonstrate continuous, (without jumps) transitions between peridotite-pyroxenite and eclogite rocks. Moreover, the compositions of minerals in diamond-forming rocks show an increasing content of Cr in peridotite garnets and jadeite component in eclogite clinopyroxenes. A large volume of mineralogical and

physicochemical experimental data allow to researchers to conclude about the existence of a certain mechanism of eclogite genesis, when minerals of peridotite and eclogite parageneses were formed sequentially as a result of ultrabasic-basic evolution of parental melts with a transition from peridotite to eclogite rocks. Generalization of analytical data on the chemical and phase compositions of rock-forming minerals of the upper mantle and paragenic inclusions in diamonds shows that they belong to a single multicomponent system-complex olivine - garnet - clinopyroxene - corundum - coesite (Litvin, 1991).

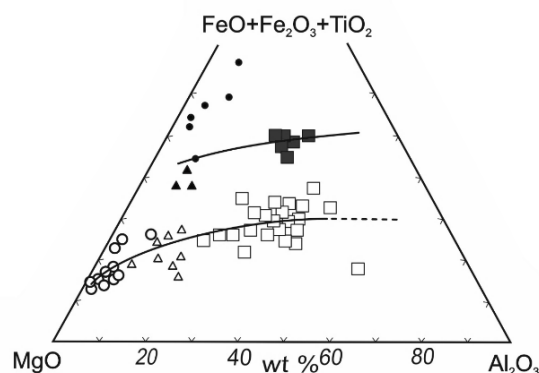


Fig. 1. Petrochemical diagram for ultrabasic and basic rocks of the upper mantle xenoliths in kimberlites according to the data of Marakushev (1984). Mg-Al rocks (white symbols): circles - garnet dunites and peridotites; triangles - garnet pyroxenites; squares - biminerall eclogites and Ky-eclogites. Fe-Ti rocks (black symbols): circles - phlogopite-ilmenite peridotites; triangles - phlogopite-ilmenite pyroxenites; squares are rutile eclogites.

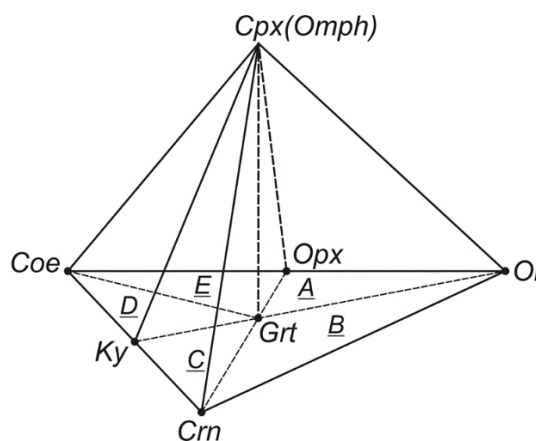


Fig. 2. Generalizing diagram-complex of compositions. It consists of ultrabasic simplexes: (A) peridotite-pyroxenitic Ol-Opx-Cpx (Omph)-Grt; (B) Ol-Crn-eclogitic Ol-Cpx (Omph)-Grt-Crn and basic simplexes: (C) Crn-Ky-eclogitic Crn-Cpx(Omph)-Grt-Ky, (D) Ky-Coe-eclogitic Ky-Cpx(Omph)-Grt-Coe, (E) Coe-Opx-eclogitic Coe-Cpx(Omph)-Grt-Opx

The diagram-complex of compositions of the upper mantle garnet-peridotite facies (Fig. 2, Litvin et al., 2016) makes it possible to study ultrabasic-to-basic petrological and mineralogical objects of the upper mantle within a single physicochemical system.

Analysis of equilibrium structure of the liquidus of Ol - Cpx - Crn - Coe system (Litvin et al., 2019) reveals the existence of temperature maxima in the Opx - Cpx(Omph) - Grt system, corresponding the "eclogite thermal barrier" (O'Hara, 1968) that separates ultrabasic and basic compositions. Therefore, ultrabasic-to-basic evolution is impossible at equilibrium conditions. But fractional crystallization of garnet lherzolite material of the upper mantle gives a physicochemical possibility of such a paragenetic peridotite-eclogite transition, it is effective in the interior of the Earth. As liquidus silicate phases crystallize, residual melts and continuous solid solutions (Cpx \leftrightarrow Omph) becomes enriched in the jadeite component, and the overall composition of the system changes from olivine-saturated rocks to silica-saturated ones.

The study of the mechanisms of ultrabasic-basic evolution of mantle systems is carried out in a physicochemical experiment using methods of physical chemistry of multicomponent multiphase systems (Rhines, 1956; Palatnik and Landau, 1961).

Experimental studies at high pressure of phase equilibria of the multicomponent peridotite-pyroxenite system olivine Ol - orthopyroxene Opx - clinopyroxene Cpx - garnet Grt showed that Opx disappears in peritectic reaction $Opx + L \rightarrow Cpx$ (Litvin, 1991). As a result, it was found that the invariant peritectic association $Ol + Opx + Cpx + Grt + L$ of the ultrabasic system is transformed into a monovariant cotectic association $Ol + Cpx + Grt + L$. Experimental studies at pressures above 4.5 GPa revealed the reaction of olivine and jadeite with the formation of garnet (Gasparik and Litvin, 1997).

The aim of this work is determination of physicochemical mechanisms of fractional ultrabasic-to-basic magmatic evolution of material of garnet-peridotite facies with a transition from olivine-containing peridotite-pyroxenite compositions to silica-saturated eclogite-grospidite compositions in both, a dry system and at fluid presence.

Experimental studies of phase relations were carried out at 6 GPa during melting of "dry"

magmatic system $Ol - (Di / Cpx) - (Jd / Omph) - Grt$ in its polythermal section $Ol - Omph (= Di_{38}Jd_{62})$ (Litvin et al., 2019). Secondary metastable phases, which were formed during the quenching solidification of the same melts as the liquidus phases, were estimated critically.

The reaction of components of olivine and jadeite-containing melt is detected with a formation of garnet and its liquidus field $Grt + L$ at temperatures not lower than 1650° C in the range of contents of Ol from ~ 40 to ~ 50 wt %, (Fig. 3). There is a quasi-invariant peritectic point $Ol + (Cpx / Omph) + Grt + L$ at temperature increasing 1380 - 1420 ° C and a content of Ol ~ 30 wt%.

At the point, after complete reactionary disappearance of olivine components ("garnetization of olivine"), a regressive monovariant cotectic $Omph + Grt + L$ appears.

Experimental studies of phase equilibria with volatile components is necessary to solve problems related to processes of melting and distribution of substance in the Earth's mantle. This allows studying their influence on the phase relationships in mantle rocks at high pressure. In this regard, the phase relations during melting of the system olivine - jadeite - diopside - garnet - volatile (C-O-H) were studied in a physicochemical experiment at a pressure of 6 GPa (conditions of the upper mantle) and temperatures of 1200-1650°C. The studies were carried out within polythermal section $Ol_{95}(C-O-H)_5 - Omph_{95}(C-O-H)_5$.

SEM photos of the samples (Fig. 4) indicate the efficiency of the peritectic reaction with Ol disappearing in the system (point "P" in the plane of the boundary ternary system $Ol - Jd - Cpx - (C-O-H)$ (Fig. 5)) as a result of the reaction. Thus, monovariant cotectic $L + Ol + Cpx / Omph + Grt$ of ultrabasic-basic system-simplex $Ol - Jd - Cpx - Grt - (C-O-H)$ in the liquidus structure (Fig. 6) serves as a kind of "physicochemical bridge" providing evolutionary transition from ultrabasic to basic magmas in the upper mantle.

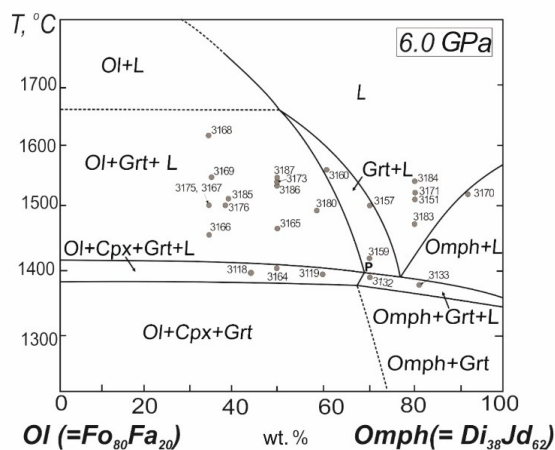


Fig. 3. Diagram of phase relations during melting of ultrabasic-basic system $Ol-Di-Jd$ in its polythermal section $Ol-Omph$

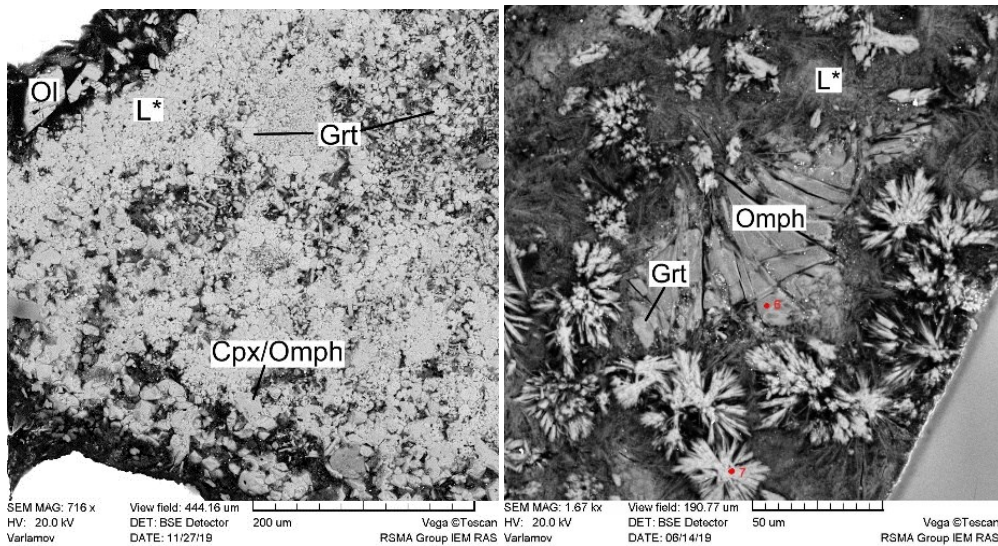


Fig. 4. Experimental samples partially melted at 6 GPa: (4a) - ultrabasic association L + Ol + Cpx / Omph + Grt with quenching phases of melt L* (sample 3233, 6 GPa, 1300°C); (4b) - basic mineral association L + Omph + Grt with quenching melt L* (sample 3223, 6 GPa, 1290°C).

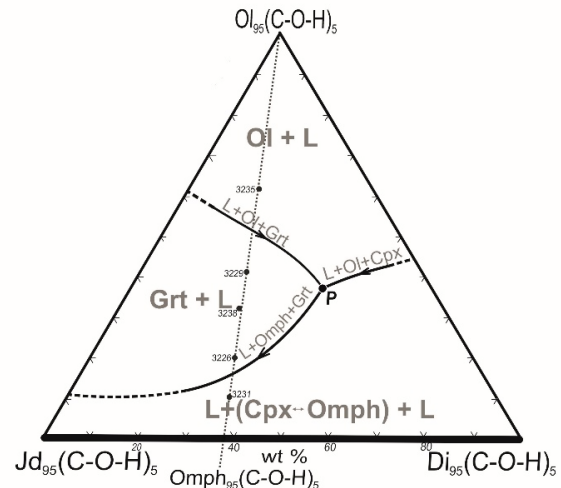
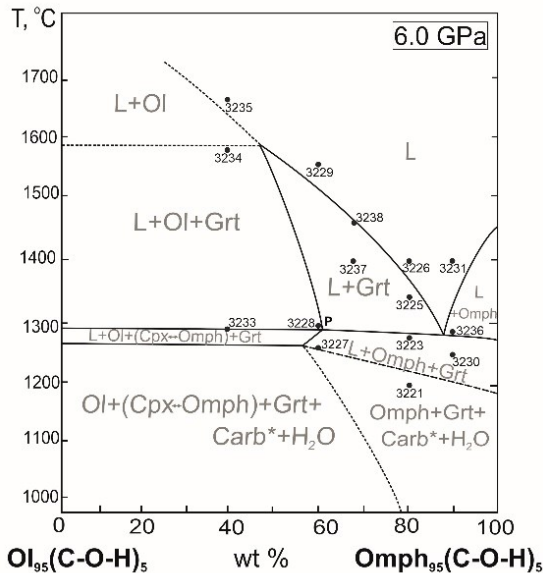


Fig. 5. Phase relations at melting within polythermal section $Ol_{95}(C-O-H)_5$ - $Omph_{95}(C-O-H)_5$ of the ultrabasic-basic system Ol - Jd - Di - Grt - (C-O-H) at 6.0 GPa.

Fig. 6. Liquidus structure of the ultrabasic-basic system Ol - Jd - Di - Grt - (COH) with reactional Grt. A participation of fluids in composition of the Ol - Jd - Di - Grt - (COH) system leads to quantitative topological changes of the parameters of its liquidus structure - a decrease in the temperatures of the solidus and liquidus boundaries, respectively, by 120 and ~ 60-80°C, as well as a shift of the composition of the peritectic reactions of olivine with increasing concentrations of olivine Mg- and Fe-components by ~ 10 wt. %.

Phase reactions at presence of C-O-H volatiles are characterized by metasomatic CO_2 -carbonatization of silicates and dissolution of H_2O in formed completely miscible silicate-carbonate melts. At the same time, the influence of C-O-H-fluid (at its content of 5 wt% with equimolecular amounts of H_2O and CO_2) on composition and temperature of the quasi-invariant peritectic reaction of olivine and jadeite-containing melt with formation of garnet was found.

Since the used concentrations of (C-O-H)-fluid components do not introduce radical qualitative changes in the phase relations during the melting of

the ultrabasic-basic system olivine - jadeite-diopside - garnet - volatile (C-O-H) at 6 GPa, the peritectic reaction of olivine remains of paramount importance. It is the main element of the liquidus structure of magmatic silicate-fluid and diamond-forming silicate-carbonate-carbon-fluid systems. The value of this reaction is in its control of final stages of ultrabasic-to-basic evolution of magmatic and diamond-forming melts of the upper mantle.

The work was carried out at financial support of theme of research plan of the IEM RAS AAAA-A18-118020590140-7

- Sobolev N. V. Deep-seated inclusions in kimberlites and the problem of the composition of the upper mantle. – American Geophysical Union, 1977.
- MacGregor, Carter. The chemistry of clinopyroxenes and garnets of eclogite and peridotite xenoliths from the Roberts Victor mine, South Africa // *Physics of the Earth and Planetary Interiors*. – 1970. - V. 3. - P. 391-397.
- Marakushev A. A. Peridotite nodules in kimberlites as indicators of the deep structure of the lithosphere / *Reports of Soviet geologists at the XXVII session of the International Geological Congress. Petrology*. – 1984. - P. 153-160 (in Russian).
- Litvin Yu. A. Physicochemical studies of the melting of the deep-seated matter of the Earth. Moscow: Science, 1997 (in Russian).
- Litvin Yu. A., Spivak A. V., Kuzyura A. V. Foundations of the mantle-carbonatite concept of diamond genesis // *Geochemistry International*. –2016. -V. 54. -№ 10. - P. 839-857.
- O'Hara M. The bearing of phase equilibria in synthetic and natural systems on the origin and evolution of basic and ultrabasic rocks // *Earth-Sci. Rev.* -1968. -V. 4. - P. 69-133.
- Rhines F. N. Phase diagrams in metallurgy: their development and application. -McGraw-Hill Companies, 1956.
- Palatnik L. S., Landau A. I. Phase equilibria in multicomponent systems. -Publishing house of the Kharkov state. Univ, 1961 (in Russian).
- Gasparik T., Litvin Yu. A. Stability of $\text{Na}_2\text{Mg}_2\text{Si}_2\text{O}_7$ and melting relations on the forsterite-jadeite join at pressures up to 22 GPa // *European Journal of Mineralogy*. -1997. -V. 9. № 2. -P. 311-326.
- Litvin Yu. A., Kuzyura A. V., Limanov E. V. The role of garnetization of olivine in the olivine–diopside–jadeite system in the ultramafic–mafic evolution of upper-mantle magmatism (experiment at 6 GPa) // *Geochemistry*. -2019. -V. 57. -P. 1045-1065.

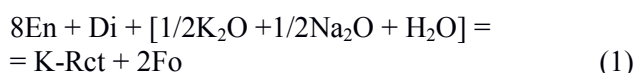
Limanov E.V., Butvina V.G., Safonov O.G., Van K.V., Vorobey S.S. K-richterite formation in the presence of K_2CO_3 - Na_2CO_3 - CO_2 - H_2O fluid. Experiment at 3 GPa. UDC 552.4

D.S. Korzhinskii Institute of Experimental Mineralogy Russian academy of science (IEM RAS), Chernogolovka, Moscow region (limanov.ev@iem.ac.ru).

Abstract. The reaction $8\text{En} + \text{Di} + [1/2\text{K}_2\text{O} + 1/2\text{Na}_2\text{O} + \text{H}_2\text{O}] = \text{K-Rct} + 2\text{Fo}$ was studied experimentally the presence of a K_2CO_3 - Na_2CO_3 - CO_2 - H_2O fluid a temperature of 1000°C and a pressure of 3 GPa. The amphibole formation was possible at a weight ratio $(\text{K}_2\text{CO}_3 + \text{Na}_2\text{CO}_3) / (\text{CO}_2 + \text{H}_2\text{O}) = 3/7$, at $\text{Na}_2\text{CO}_3/\text{K}_2\text{CO}_3 = 50/50$ and $70/30$. In a situation where potassium dominates over sodium, amphibole is formed only at $(\text{K}_2\text{CO}_3 + \text{Na}_2\text{CO}_3) / (\text{CO}_2 + \text{H}_2\text{O}) = 10/90$. Amphibole becomes unstable with an increase in the content of alkaline components in the fluid, a large amount of alkaline melt is present in the system. The regularities obtained in the work reproduce well the features of mineral associations and variations in component compositions in the upper mantle peridotites.

Keywords: mantle metasomatism, experiment, fluid, upper mantle, K-Richterite

Studies of xenoliths from alkaline kimberlites and basaltoids indicate the presence in the mantle of a multistage process of alteration of mantle rocks during their interaction with fluids and melts of various compositions and origins, referred to as mantle metasomatism (O'Reilly & Griffin, 2013). In the course of this process, there is a change in the mineral composition of rocks, the component composition of primary minerals, as well as the generation of new minerals, such as ilmenite, titanite, carbonates, sulfides, etc., which are not characteristic of the primary paragenesis. A typical mineral indicator of modal mantle metasomatism is phlogopite, the formation of which is accompanied by the decomposition of alumina-containing minerals such as garnet and spinel. A further increase in the activity of alkaline components in the fluid leads to the decomposition of pyroxenes and the formation of K-richterite (Aoki, 1975; Erlank et al., 1986), a specific low-alumina alkaline amphibole that is stable over a wide range of temperatures and pressures (Trønnes, 2002). Its generation occurs during the reaction



with the participation of aqueous-carbonic fluids containing salt components. We carried out an experimental study in the enstatite-diopside system in the presence of the K_2CO_3 - Na_2CO_3 - CO_2 - H_2O fluid, at a temperature of 1000 °C and a pressure of 3 GPa. 3 series of experiments were carried out, differing in the ratio of Na_2CO_3 and K_2CO_3 by weight: I - 50:50; II - 70:30, III - 30:70 and the total content of alkaline components to the H_2O - CO_2 fluid. The work was carried out at the Institute of Experimental Mineralogy, IEM RAS, using a high-pressure anvil with a hole NL-40.

In the first series of experiments, the formation of amphibole was found to be possible when the ratio $(\text{K}_2\text{CO}_3 + \text{Na}_2\text{CO}_3) / (\text{H}_2\text{O} + \text{CO}_2) = 30/70$ by weight. Along with the newly formed amphibole, olivine, a by-product of reaction (1), is present among the experimental products. An increase in the activity of alkalis in the fluid leads to a decrease in the tremolite component in amphibole, which is accompanied by a change in the calcium content of both pyroxenes (Fig. 1 a). The amphibole composition shifts towards K-richterite. The high activity of alkaline components in the fluid leads to the retention of clinopyroxene mainly in the form of inclusions in olivine.

In the second, sodium series of experiments ($\text{Na}_2\text{CO}_3 / \text{K}_2\text{CO}_3 = 70/30$), amphibole is also formed at the ratio $(\text{K}_2\text{CO}_3 + \text{Na}_2\text{CO}_3) / (\text{H}_2\text{O} + \text{CO}_2) =$

30/70 by weight (Fig. 2 a). Its appearance, similar to the first series, is accompanied by a change in the calcium content of both pyroxenes, as well as the formation of olivine. The composition of amphibole shifts towards richterite, which is accompanied by an increase in its calcium content and a decrease in the amount of potassium (Fig. 1b) with an increase in alkaline components in the fluid. At high contents of alkaline components, ($K_2CO_3 + Na_2CO_3$) = 60/40, amphibole is unstable, its place is taken by an alkaline melt. The composition of the only large quenched grain of amphibole found under these conditions is shown in the graph (Fig. 2b).

At $K_2CO_3 / Na_2CO_3 = 70/30$, the formation of amphibole turned out to be possible only when the ratio $(K_2CO_3 + Na_2CO_3) / (CO_2-H_2O) = 10/90$. With an increase in the alkalinity of the fluid, amphibole occurs exclusively in the form of needles up to 2 micron in size, which characterizes it as a quenching phase (Fig. 2b). The instability of K-rich richterite can be caused by the complicated entry of a large potassium ion into the amphibole structure. Among the experimental products, the association of pyroxenes with olivine is stable.

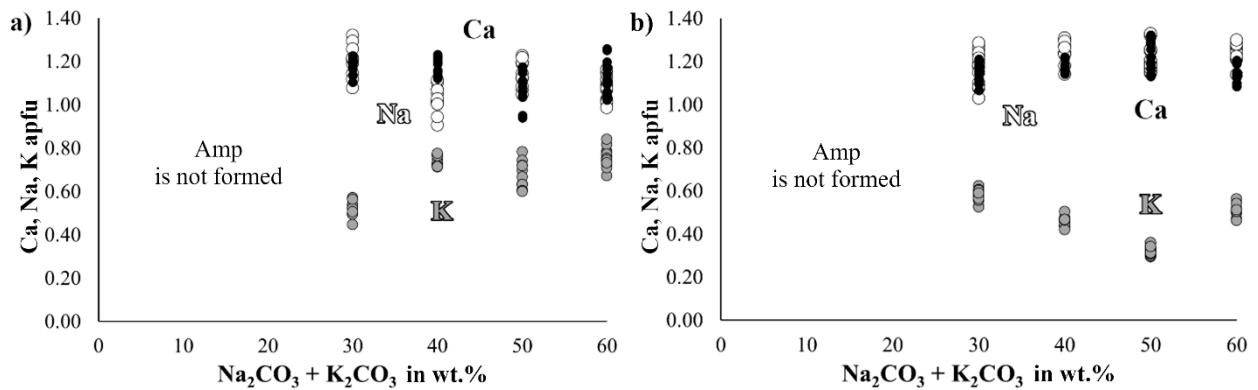


Fig. 1. Amphibole composition depending on the content of $Na_2CO_3 + K_2CO_3$ in the fluid: a) in the first series of experiments ($K_2CO_3 / Na_2CO_3 = 50/50$); b) in the second series II ($K_2CO_3 / Na_2CO_3 = 30/70$).

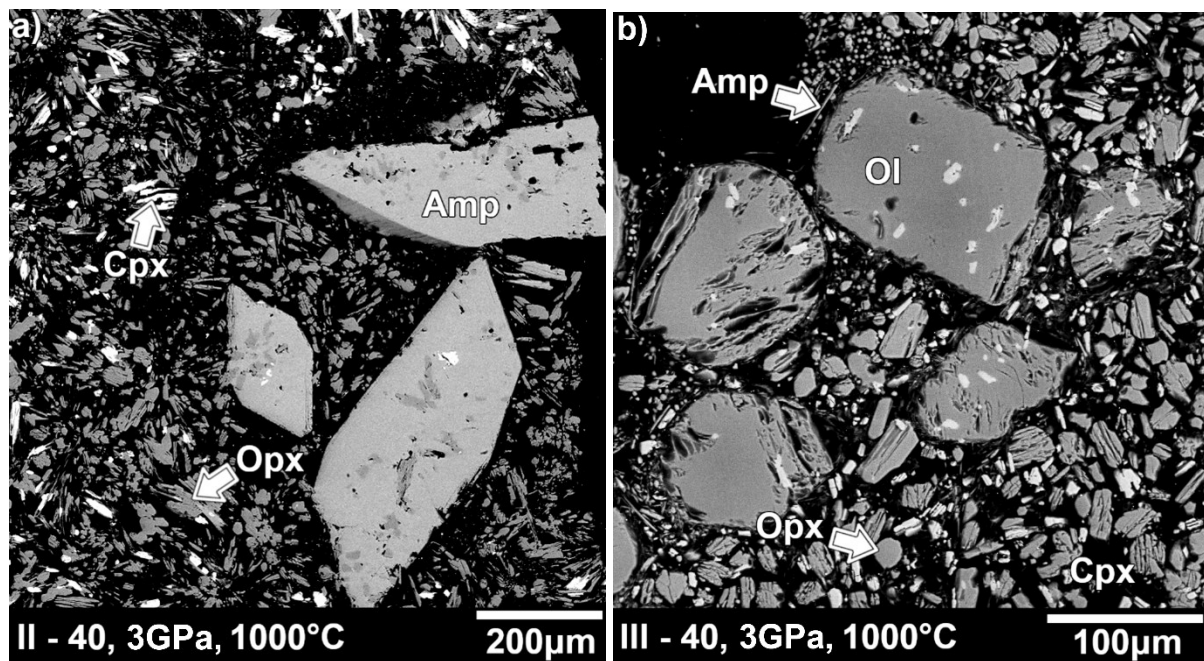


Fig. 2. Images of experimental samples in reflected electrons with the ratio $(K_2CO_3 + Na_2CO_3) / (H_2O + CO_2) = 40/60$ in the fluid: a) a sample from the II series of experiments, b) a sample from the III series. Dark prismatic inclusions in amphibole are orthopyroxene, light inclusions in olivine and amphibole are clinopyroxene.

Extreme contents of K_2O and Na_2O in the fluid lead to the generation of an alkaline melt rather than amphibole. The most favorable environment for the formation of K-rich richterite was the situation in which K_2O coexists in the fluid with Na_2O in equal proportions. The complexity of the formation of K-

richterite in the experiment, indirectly determines its rare occurrence in natural xenoliths. The obtained regularities reproduce well the features of mineral associations and variations in the component compositions in the upper mantle peridotites. The study of such changes is important for assessing the

activity of alkaline components in the fluid and pressure during modal mantle metasomatism.

References

- Aoki, K. Origin of phlogopite and potassic richterite bearing peridotite xenoliths from South Africa // Contributions to Mineralogy and Petrology – 1975. – Vol. 53. – №3. – P.145–156.
- Erlank, A. J., Waters, F. G., Haggerty, S. E., & Hawkesworth, C. J. Characterisation of metasomatic processes in peridotite nodules contained in kimberlite. // International Kimberlite Conference: Extended Abstracts – 1986. – Vol. 4 – №1. – P. 232-234.
- O'Reilly S.Y., & Griffin W.L. Metasomatism and the chemical transformation of rock. – Springer: Berlin-Heidelberg, 2013. – P. 471-533.
- Trønnes, R. G. Stability range and decomposition of potassic richterite and phlogopite end members at 5-15 GPa. // Mineralogy and Petrology. – 2020. – Vol. 74 – № 2-4. – P. 129–148.

Sokol A.G.¹, Zaikin P.A.², Zaikina O.O.³, Sokol I.A.¹ Formation of organic molecules at high pressures and temperatures: experimental constraints UDC 552.112

¹IGM SB RAS, Russian Federation, Novosibirsk, ²NIOCH SB RAS, Russian Federation, Novosibirsk, ³BIC SB RAS, Russian Federation, Novosibirsk, (sokola@igm.nsc.ru, ihatealc@gmail.com, omironenko@catalysis.ru, zaikin@nioch.nsc.ru) Corresponding author: sokola@igm.nsc.ru

Abstract. Experiments at high pressures and temperatures make it possible to reproduce the processes that determine the formation of organic molecules under the conditions of the Earth's mantle. In a first approximation, we reconstructed the chemical processes associated with the formation of hydrocarbons at P-T- fO_2 parameters close to the conditions in the mantles of terrestrial planets. The available data unambiguously confirm the formation of hydrocarbons by hydrogenation of various carbon sources under conditions with low oxygen fugacity. Carbonates, carbon dioxide, elemental carbon in the form of diamond, graphite or amorphous carbon, and finally metal carbides can act as sources for the formation of hydrocarbons. Under low fO_2 and high fH_2 conditions, the formation of light linear alkanes predominates. With an increase in fO_2 , the condensation of light alkanes into heavier ones begins. The presence of metal oxides stimulates isomerization and dehydrocyclization, leading to the formation of branched alkanes and arenes. In nitrogen-bearing systems, methanimine is formed, an aza-analog of formaldehyde, which can participate in the formation of amino acids, alternatively to the formaldehyde pathway.

Keywords: mantle; subduction; fluid; hydrocarbons; water; carbon dioxides

Recently, there has been a significant increase in interest in the reconstruction of the role of hydrocarbon fluid in mantle mineral forming processes. This is because in a number of works, including in the works of N.V. Sobolev with co-authors (Sobolev et al., 2018, 2019a, 2019b;

Tomilenko et al., 2018) hydrocarbons were found in inclusions in diamonds and deep minerals from the kimberlites of Yakutia, as well as in diamonds from the Urals placers. They were also found in ultra-deep diamonds (Smith et al., 2016). Thermodynamic calculations and experiments with organic matter confirm the stability of hydrocarbons in the mantle fluid at fO_2 below the carbon-saturated "water maximum" (Stachel and Luth, 2015; Sokol et al., 2017a, 2017b). The model developed Stachel and Luth (2015) links the genesis of the diamond with the interaction of depleted peridotites of the subcratonic mantle with the ascending hydrocarbon fluids.

This article summarizes the data of our experiments performed in the multi-anvil apparatus BARS at pressures of 5.5-7.8 GPa and temperatures of 1000-1400°C. In the first series of experiments, we used natural graphite (99.99% C), which contained 53 ppm Fe, 9 ppm Mo, and trace quantities of other elements according to ICP-MS data (Sokol et al., 2019a). The graphite was dried at 110°C for at least 30 days. An amorphous carbon ¹³C (99%, Cambridge Isotope Laboratories, Inc.) used in several experiments was annealed at 1000°C for 10 hours in the flow of helium. Synthetic diamond (ACM-20/14, 14-20 microns) was annealed in air for 1 hour at 700°C. The starting materials were placed in 2 mm diameter capsules made of Pt or Au.

In the second series of experiments, mixtures of graphite with Fe, Ni, or Fe₃C were used (all reagents of >99.99% purity). Iron and nickel powders (10-50 microns) were pre-cleaned by annealing in hydrogen flow for 1 hour at 600°C. Fe₃C was synthesized at 6.3 GPa and 1400°C. Carbon-poor samples were placed in Al₂O₃ containers, and carbon-rich samples in graphite containers. The containers then were placed in Pt or Au capsules with a diameter of 2 mm. All capsules were hermetically sealed with high-frequency pulse arc welding using PUK-4U apparatus (Lampert Werktechnik GmbH, Germany). It is important to note that organic substances were not used in our experiments.

Two-capsules technique was used to control hydrogen fugacity (fH_2) in the samples. In the outer thick-walled capsules made of Fe or Mo talc was placed as a water source. A reaction of water with Fe or Mo provided hydrogen generation at the level of IW+H₂O (iron – iron (II) oxide) or MMO+H₂O (molybdenum – molybdenum (IV) oxide) buffers.

The analysis of quenched fluids was performed by gas chromatography/mass-spectrometry method using Thermo Scientific Focus GS/DSQ II Series single quadrupole MS instrument (IGM SB RAS). For special tasks (determining the molecular formula of fluid components) a high-resolution mass spectroscopy Thermo Fisher Scientific Double Focusing System (DFS), (NIOC SB RAS) was used.

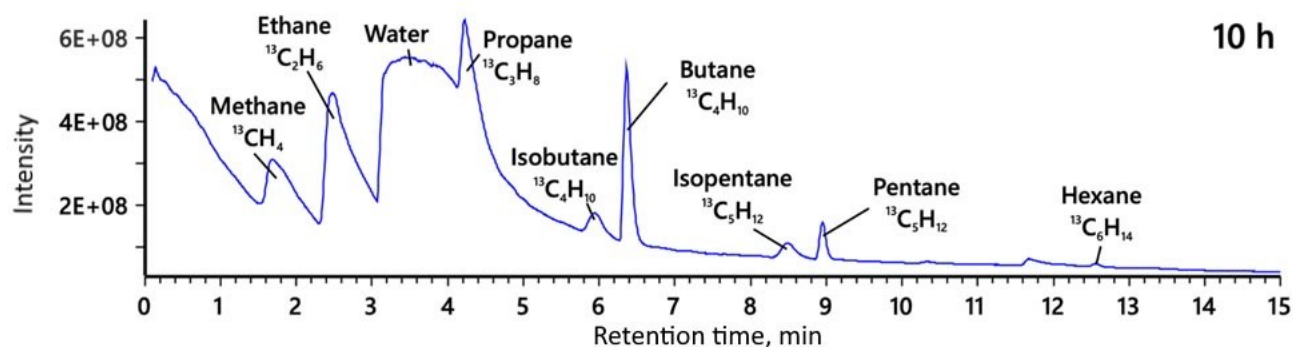


Figure 1. Fragment of total ion chromatogram (TIC) of quenched fluid obtained in a 10-hour experiment.

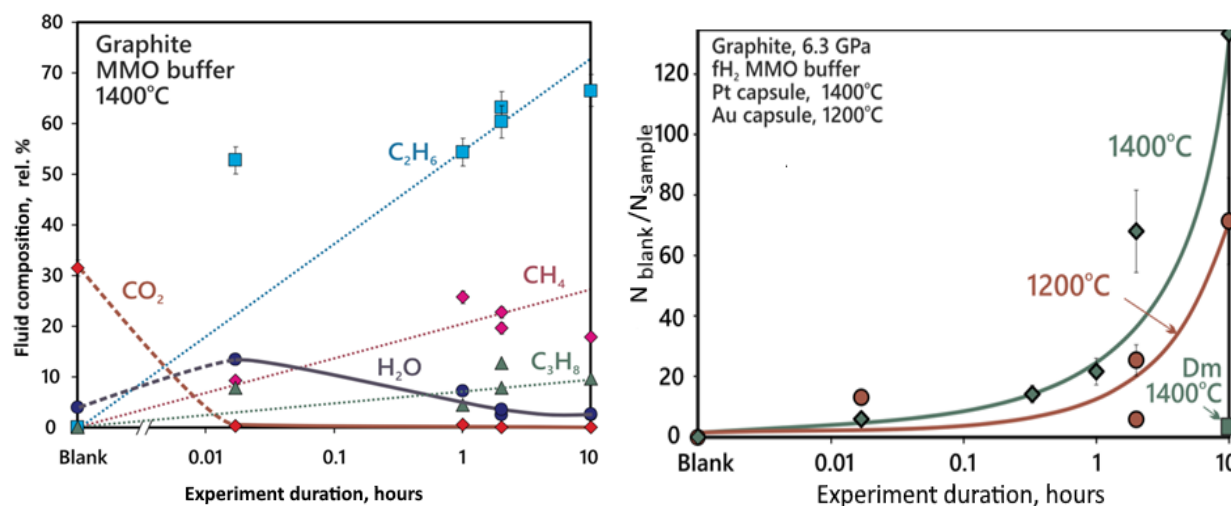


Figure 2. The compositions of quenched fluids from experiments with graphite in Pt ampules at 1400°C

Figure 3. The nitrogen content of quenched fluids from experiments with graphite in Pt ampules at 1400°C

In the first series we performed the experiments to investigate the interaction of ^{13}C amorphous carbon with fluid at 6.3 GPa and 1200°C and controlled f_{H_2} . For the first time an isotopically pure alkanes were obtained in the experiments. The presence of ^{13}C -alkanes (Fig. 1) proves the possibility of direct synthesis of hydrocarbons from inorganic starting materials and excludes even local contamination of the samples by organic ^{12}C substances. After the first experiment performed at 2GPa and room temperature only small amounts of adsorbed gases were extracted from ampules. After the second experiment of 1 min duration conducted at 6.3 GPa and 1200°C we detected a desorption of CO_2 and H_2O and start of synthesis of hydrocarbons. After the third experiment of 10 hours duration at the same P-T parameters large quantities of ^{13}C -alkanes and iso-alkanes were formed along with significant amount of water generated possibly by the CO_2 reduction (Fig. 1).

Figure 2 demonstrates the compositions of fluids obtained by graphite hydrogenation at 6.3 GPa and 1200-1400 °C. Light alkanes ($\text{C}_2 > \text{C}_1 > \text{C}_3 > \text{C}_4$)

dominate in fluids generated in Pt capsules at 1200-1400 °C. The methane to ethane ratio $\text{CH}_4/\text{C}_2\text{H}_6 > 1$ was observed in all experiments carried out in Au capsules at 1200°C. We propose that Pt can catalyze the methane dimerization on the heated capsule walls at high methane partial pressure in the sample. The kinetics of hydrocarbons formation by the graphite or diamond hydrogenation was investigated by the method of dilution of atmospheric nitrogen trapped during the capsule assembly. In the hydrogenation of graphite at 1200 and 1400 °C an avalanche-like increase of quantities of light alkanes with an increase in the duration of the experiment was observed. An increase in pressure was found to lead both to an increase in the absolute yield of HCs and to chain elongation of HC products. At the same time, the rate of hydrocarbons production in the hydrogenation of diamonds was much slower than in experiments with the hydrogenation of graphite. Experiments with added H_2O or H_2^{18}O demonstrated that water does not participate in the generation of hydrocarbons at the experimental P-T- f_{H_2} parameters.

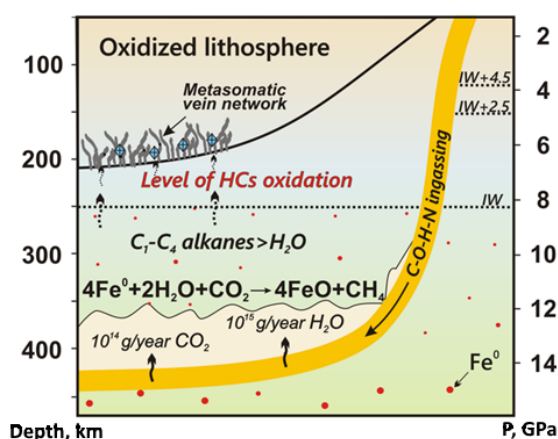


Figure 4. The model of the formation of hydrocarbons by the interaction of subducted fluids with metal-containing mantle.

The formation of hydrocarbons by the interaction of fluid with iron and iron carbide was investigated at 6.3 GPa and 1000-1400 °C. In the experiments of the second series, it is established that the reactions of iron or iron carbide with water fluid provide fH_2 necessary and sufficient for the synthesis of hydrocarbons at mantle P-T parameters. At 6.3 GPa and 1200 °C the CH_4/C_2H_6 ratio in quenched fluids decreases with the increase in carbon concentration and the decrease in iron content in the system. At the same time, the total amount of fluid is increasing.

Currently, the processes of hydrocarbon formation are also being actively studied using diamond anvils, including the works of V. Kucherov's group (Kucherov et al., 2020, Serovaiskii and Kucherov, 2021). Comparison of the methods used in various high-pressure apparatuses shows that each of the approaches has its own strengths and weaknesses. In particular, the experiments in diamond anvils allow *in situ* analysis of the fluid composition, but there is no possibility to buffer fH_2 . The formation of a small amount of fluid makes it difficult to analyze its composition by traditional analytical methods, such as chromatographic methods. The main drawback of the experiments in cells of multi-anvil apparatus is the necessity to quench the fluid before its analysis. Generalization of the data collected in our experiments shows that high fH_2 promotes the synthesis of light linear hydrocarbons C_1-C_6 at mantle P-T parameters. In diamond anvils, due to the diffusion of hydrogen outside the sample, with an increase in fO_2 , a condensation of light alkanes into heavier ones is observed. The presence of metal oxides stimulates isomerization and dehydrocyclization, leading to the formation of branched alkanes and arenes.

In connection with the development of a deep nitrogen cycle, it becomes important to study the stability of nitrogen-bearing components of mantle fluids. As shown earlier in our work (Sokol et al., 2017b), at mantle P-T parameters, N_2 is stable in

oxidized nitrogen-rich fluids, while NH_3 is stable in strictly reduced fluids, at redox conditions of IW buffer. At the same time, methanimine (CH_3N), an aza analog of formaldehyde, was detected for the first time using GC-MS and high-resolution mass spectroscopy in a nitrogen-poor C-O-H-N fluid obtained at 6.3 GPa and 1000-1200°C and high fH_2 (Sokol et al., 2019b). The experimentally detected mass of a molecular ion ($M + m/z$: 29.0250) is close to the calculated one ($M + m/z$: 29.0260).

The paper summarizes the experimental data important for the reconstruction of hydrocarbon formation processes in the mantle (Fig. 4). The reaction of H_2O -containing subduction fluids with a metal-saturated mantle provides sufficient fH_2 for the formation of hydrocarbons. Graphite, diamond and iron carbide, which are required for the synthesis of hydrocarbons, can be generated by the interaction of native iron with carbonates or CO_2 . Hydrogenation of graphite, diamond and iron carbide can provide the synthesis of hydrocarbons at mantle P-T parameters. The ratio of the amounts of $H_2O + CO_2$ subducted into the mantle, as well as metallic Fe in the slab-mantle interaction zones, could determine the scale and duration of the generation of hydrocarbons by this mechanism. Apparently, it could function for a relatively short time, immediately after the beginning of the subduction of the oceanic crust to the mantle depths. The data obtained allowed us to formulate the following conclusions. Reactions of fluid with phases simulating the composition of native iron and carbon sources (graphite, amorphous carbon, diamond, etc.) under P-T- fH_2 conditions of the reduced mantle can provide the generation of complex hydrocarbon systems, mainly consisting of light alkanes. The concentration of carbon and metallic iron in model systems significantly affects the composition of the resulting alkanes. Conditions favorable for the formation of hydrocarbons exist in zones in which H_2O -, CO_2 -bearing subduction fluids interact with the metal-saturated mantle. Methane imine (CH_3N) may be an important component of nitrogen-poor mantle fluids.

Work is done on state assignment of IGM SB RAS. The authors are grateful to A.A. Tomilenko, T.A. Bulbak and A.A. Nefedov for cooperation.

References

- Smith E.M., Shirey S.B., Nestola F., Bullock E.S., Wang J., Richardson S.H. and Wang W. Large gem diamonds from metallic liquid in Earth's deep mantle // *Science*. – 2016. – Vol. 354. – P. 1403–1405.
- Sobolev N.V., Logvinova A.M., Tomilenko A.A., Wirth R et al. Mineral and fluid inclusions in diamonds from the Urals placers, Russia: Evidence for solid molecular N_2 and hydrocarbons in fluid inclusions // *Geochim. Cosmochim. Acta*. – 2019a. – Vol. 266. – P. 197–219.

- Sobolev N.V., Tomilenko A.A., Bul'bak T.A., Logvinova A.M. Composition of hydrocarbons in diamonds, garnet, and olivine from diamondiferous peridotites from the Udachnaya pipe in Yakutia, Russia // *Engineering*. – 2019b. – Vol. 5. – P. 471–478
- Sokol A.G., Tomilenko A.A., Bul'bak T.A., Palyanova G.A. et al. Carbon and Nitrogen Speciation in N-poor C-O-H-N Fluids at 6.3 GPa and 1100–1400°C // *Sci. Rep.* – 2017a. – Vol. 7. – P. 1–19.
- Sokol A.G., Palyanov Y.N., Tomilenko A.A., Bul'bak T.A., Palyanova G.A. Carbon and nitrogen speciation in nitrogen-rich C-O-H-N fluids at 5.5–7.8 GPa // *Earth Planet. Sci. Lett.* . – 2017b. – Vol. 460. –P. 234–243.
- Sokol, A. G., Tomilenko, A. A., Bul'bak, T. A., Sokol, I. A. et al. Hydrogenation of carbon at 5.5–7.8 GPa and 1100–1400 C: Implications to formation of hydrocarbons in reduced mantles of terrestrial planets // *Phys. Earth Planet. Int.* – 2019. – Vol. 291. – P. 12–23.
- Sokol A.G., Tomilenko A.A., Sokol I.A., Zaikin P.A., Bul'bak T.A. Formation of hydrocarbons in the presence of native iron under upper mantle conditions: Experimental constraints // *Minerals*. – 2020. – Vol. 10(2) . – P. 88.
- Sokol I.A., Sokol A.G., Bul'bak T.A., Nefyodov, A.A. et al. C-and N-bearing species in reduced fluids in the simplified C–O–H–N system and in natural pelite at upper mantle P–T conditions // *Minerals*. – 2019. – Vol. 9(11) . – P. 712.
- Tomilenko A.A., Bulbak T.A., Logvinova A.M., Sonin V.M., Sobolev N.V. The composition features of volatile components in diamonds from the placers in the northeastern part of the Siberian Platform by gas chromatography-mass spectrometry // *Dokl. Earth Sci.* – 2018. – Vol. 481 (1) . – P. 953–957.

Spivak A.V.¹, Borovikova E.Yu.², Setkova T.V.¹, Zakharchenko E.S.¹ Raman spectroscopy of synthetic brunogeierite (Fe₂GeO₄) at pressure up to 30 GPa UDC 543.42

¹IEM RAS(Chernogolovka), ²Lomonosov MSU (Moscow) spivak@iem.ac.ru

Abstract. For synthetic brunogeierite, Raman spectroscopic study was carried out at pressures up to 30 GPa using a diamond anvil cell. The Raman spectra of Fe₂GeO₄ crystal consist of an intense main band at 756 cm⁻¹ and three less intense bands at ~ 644, 302, and ~ 205 cm⁻¹ at normal conditions. All five bands inherent in the spectrum of cubic spinel could be traced in high pressure spectra. A gradual change in the Raman spectra is observed at high pressure. This allows us to conclude that there is no sharp rearrangement of the structural type under pressure up to 30 GPa.

Keywords: spinel, germanium, germanate, Raman spectroscopy, high pressure, lattice dynamic calculations, phase transition

Brunogeierite is a rarely occurring mineral with spinel structure. The ideal end-member formula of

brunogeierite was redefined as Fe²⁺₂Ge⁴⁺O₄ (Cempírek, Groat, 2013) on the basis of bond-valence calculations carried out using a structural model of brunogeierite obtained with single-crystal X-ray diffraction data (Welch et al., 2001).

The geochemical similarity of silicon with germanium makes it possible to use germanium analogs of silicate minerals as high-pressure models for studying phase relations. Chemical deformations that can occur in the structures of silicate phases when a larger Ge cation enters are equivalent to changes in structures under high pressure. Insofar as, the spinel Mg₂GeO₄ is analogue of high-pressure ringwoodite γ-Mg₂SiO₄. The brunogeierite Fe₂GeO₄ is also analogue of ahrensite γ-Fe₂SiO₄, and can be used to model high-pressure behavior of the latter.

The goal of this work is *in situ* Raman spectroscopic study of synthetic brunogeierite at pressures up to 30 GPa, determination of possible phase transitions using experimental data, factor-group analysis of vibrations, and lattice dynamics calculation based on the structural data of brunogeierite.

Synthetic crystals of brunogeierite up to 500 μm in size were obtained in an autoclave as a result of the interaction of a boric acid solution on a iron wire in the presence of germanium oxide (GeO₂) at a temperature of 600 °C and a pressure of 100 MPa at the IEM RAS.

The chemical compositions of experimental samples were determined by electron microprobe analysis (EMPA) with using Tescan - VegaIIXMU electron microscopy with INCA Energy 450 energy dispersive spectrometer (EDS), equipped with an INCA x-sight semiconductor Si(Li) detector and an INCA Wave 700 wavelength-dispersive spectrometer (WDS) (Oxford Instruments) at IEM RAS.

Raman spectra of the experimental samples at high-pressure were measured using the apparatus consisting of spectrograph Acton SpectraPro-2500i with detector cooling up to -70 °C CCD Pixis2K and the microscope Olympus with a continuous solid-state monomeric laser with radiation wavelength 532 nm and diode pumping at IEM RAS. The laser beam diameter was 3–5 μm. Raman data were collected by repeated exposures of 540 s (3 × 180 s). High-pressure Raman-spectroscopy experiments were carried out in a diamond anvil cell (DAC) up to 30 GPa with 1–2 GPa step. NaCl was used as a pressure medium. The software Fytik 1.3.1. was used for profile fitting for the Raman band analysis.

The Fe₂GeO₄ phase crystallizes with a space group *Fd* $\bar{3}$ *m* with spinel structure. Factor-group analysis suggests five Raman-active vibration modes are allowable for oxide spinels, with the following symmetries A_{1g} + E_g + 3F_{2g}. The Raman spectra of synthetic brunogeierite crystal (Fig. 1) consist of a

major intensiv band at 756 cm^{-1} . Other minor bands are seen near ~ 644 , 302 and $\sim 205\text{ cm}^{-1}$. Bands $\sim 756\text{ cm}^{-1}$ (A_{1g}) and $\sim 644\text{ cm}^{-1}$ (F_{2g}) correspond to symmetric (ν_1) and asymmetric (ν_3) stretching motions of the tetrahedral GeO_4 units by analogy to SiO_4 groups in ringwoodite $\gamma\text{-Mg}_2\text{SiO}_4$. The 302 cm^{-1}

band is assigned to symmetric vibrations (E_g) of GeO_4 .

Figure 1 shows the Raman spectra for natural and synthetic brunogeierite in comparison with ahrensite and Ge-ringwoodite at normal conditions.

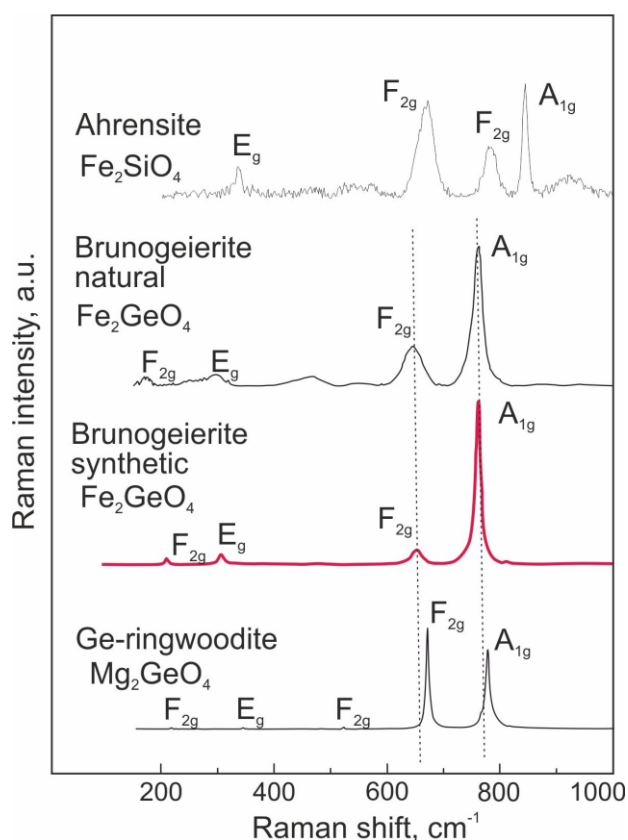


Fig. 1. Raman spectra Fe^{2+} and/or Ge^{4+} $\text{A}^{2+}_2\text{B}^{4+}_4\text{O}_4$ spinel. Ahrensite $\gamma\text{-Fe}_2\text{SiO}_4$ (<https://rruff.info/X050109>); nature brunogeierite Fe_2GeO_4 (<https://rruff.info/%20R090012>); synthetic brunogeierite Fe_2GeO_4 (this work); Ge-ringwoodite $\gamma\text{-Mg}_2\text{GeO}_4$ (Thomas et al., 2008).

Previously the cubic spinel Fe_2GeO_4 has not been investigated under the high-pressure conditions. Possible structural distortion of Fe_2GeO_4 has been investigated below the Néel temperature. Structural transitions were not detected down to $T \sim 8\text{ K}$ (Barton et al., 2014).

Other cubic germanium spinels demonstrate different behavior under high pressure conditions, which was summarized at (Yamanaka et al., 2008). Co_2GeO_4 and Ni_2GeO_4 spinels decompose into their isochemical oxide mixtures at about 250 kbar and $1400\text{-}1800^\circ\text{C}$. Mg_2GeO_4 at atmospheric pressure occurs in two polymorphic modifications: olivine-type and cubic spinel type. The post-spinel transformations of Mg_2GeO_4 are expected (Ilmenite $\text{MgGeO}_3 + \text{MgO}$ or/and perovskite + MgO).

The crystal $\gamma\text{-Fe}_2\text{SiO}_4$ is the most similar by chemical compound to brunogeierite. The phase transition at about 30 GPa supposed to the rhombohedral distortion of cubic structure (Greenberg et al., 2011), but the orthorhombic crystal

structure (*Imma* space group) was identified at about 34 GPa, characterizing by the changing of coordination number of silicon atoms from 4 to 6 (Yamanaka et al., 2015).

The Raman spectroscopy could be powerful tool for structural distortion investigations. The Raman spectra of synthetic brunogeierite single crystal under the pressures up to 30 GPa are shown on the figure 3. At the low pressures (1-2 GPa) the band of asymmetrical bending vibrations of GeO_4 tetrahedron becomes apparent at $\sim 475\text{ cm}^{-1}$. All five bands inherent in the spectrum of cubic spinel could be traced in high pressure spectra. Four of them shift to higher wavenumbers reflecting the decreasing of interatomic distances. The band at $\sim 220\text{ cm}^{-1}$ is very stable in frequency. The gradually changing of Raman spectra is observed, so we can conclude the absence of abrupt rebuild of structural type. Ge obviously stay tetrahedrally coordinated till 30 GPa. But we observed some extra bands at the spectra obtained at high pressure (Fig. 3).

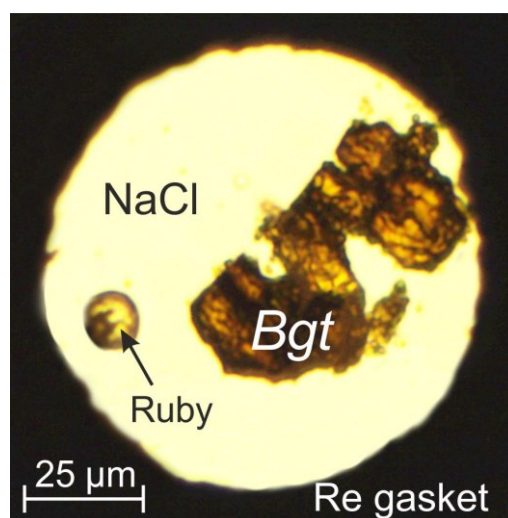


Fig. 2. Image of experimental volume in a rhenium gasket with a brunogeierite sample (*Bgt*) and pressure sensor (ruby) at 4.2 GPa.

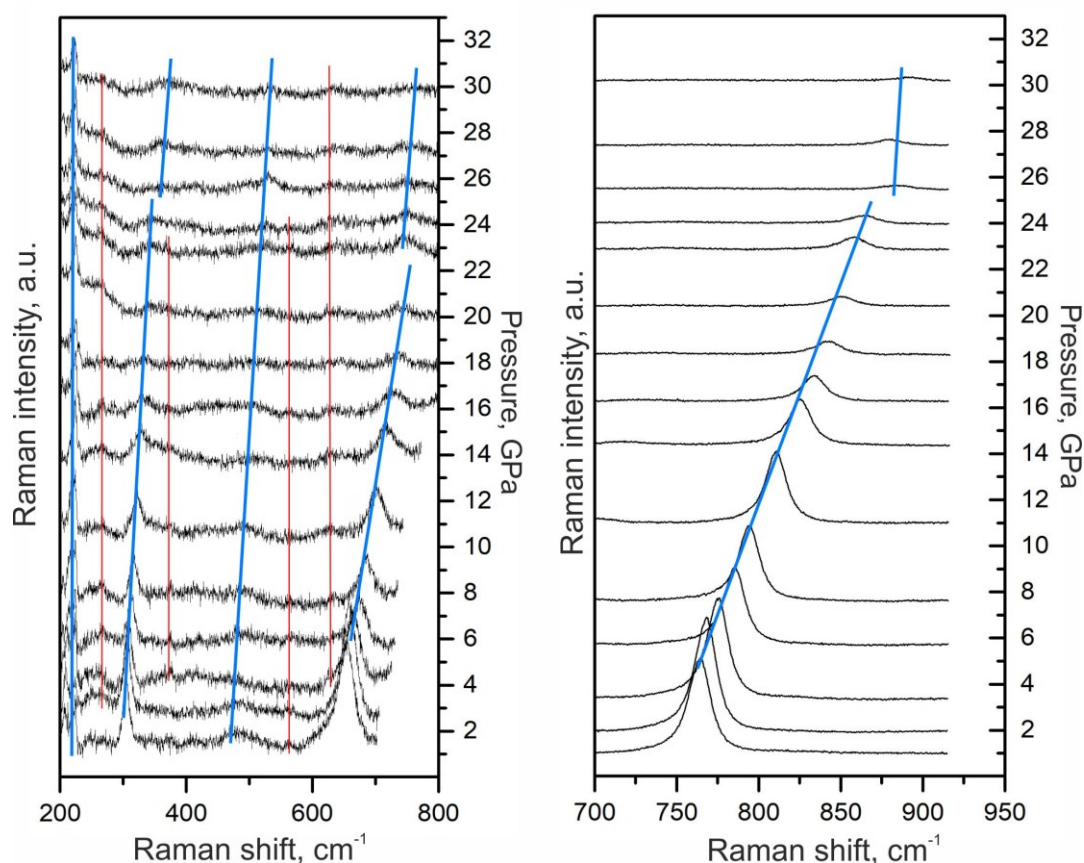


Fig. 3. Raman spectra of synthetic brunogeierite Fe_2GeO_4 at high pressure and ambient temperature. Blue lines – trends of shifting of the main five bands for Raman spectrum of cubic spinel, red lines - trends of shifting of additional bands.

High pressure Raman spectroscopy studies of various spinels have shown that during the transition from one modification to another or decomposition in situ, two phases or the initial phase and decomposition products can coexist in a wide pressure range (up to $\Delta = 16$ GPa) (Wang et al., 2020; Wang et al., 2002, 2003). This process is observed in the Raman spectrum by a gradual decrease of the initial phase bands intensity and an increase of the bands intensity of the transformed phase or decomposition phases. In the Fe_2GeO_4 spectra, we observed the presence of additional bands in a wider pressure range (from 1.5 to 30 GPa). Additionally, the lattice dynamics calculation with using the structural data of brunogeierite shows the decreases cubic symmetry of the structure to tetragonal or rhombohedral in this pressure range.

This work is fulfilled under the Research Programs AAAA-A18-118020590140-7 and AAAA-A18-118020590150-6 of the Korzhinskii Institute of Experimental Mineralogy RAS.

References

- Cempírek J., L.A. Groat, Note on the formula of brunogeierite and the first bond-valence parameters for Ge^{2+} , *J. Geosci.* 58 (2013) 71–74.
- Greenberg E., L.S. Dubrovinsky, C. McCammon, J. Rouquette, I. Kantor, V. Prakapenka, G.K. Rozenberg, M.P. Pasternak, Pressure-induced structural phase transition of the iron end-member of ringwoodite (γ - Fe_2SiO_4) investigated by X-ray diffraction and Mössbauer spectroscopy, *Am. Mineral.* 96 (2011) 833–840. <https://doi.org/10.2138/am.2011.3647>.
- Thomas S.M., M. Koch-Müller, V. Kahlenberg, R. Thomas, D. Rhede, R. Wirth, B. Wunder, Protonation in germanium equivalents of ringwoodite, anhydrous phase B, and superhydrous phase B, *Am. Mineral.* 93 (2008) 1282–1294.
- Wang C.P., S.R. Shieh, A.C. Withers, X. Liu, D. Zhang, S.N. Tkachev, A.E. Djirar, T. Xie, J.D. Rummey, Raman and X-ray diffraction study of pressure-induced phase transition in synthetic Mg_2TiO_4 , *Sci. Rep.* 10 (2020) 1–12.
- Wang Z., H.S.C. O'Neill, P. Lazorc, S.K. Saxena, High pressure Raman spectroscopic study of spinel MgCr_2O_4 , *J. Phys. Chem. Solids.* 63 (2002) 2057–2061.
- Wang Z., S.K. Saxena, P. Lazor, H.S.C. O'Neill, An in situ Raman spectroscopic study of pressure induced dissociation of spinel NiCr_2O_4 , *J. Phys. Chem. Solids.* 64 (2003) 425–431.
- Welch M.D., M.A. Cooper, F.C. Hawthorne, The crystal structure of brunogeierite, Fe_2GeO_4 spinel, *Mineral. Mag.* 65 (2001) 441–444.
- Yamanaka T., A. Kyono, Y. Nakamoto, S. Kharlamova, V. V. Struzhkin, S.A. Gramsch, H.K. Mao, R.J. Hemley, New structure of high-pressure body-centered orthorhombic Fe_2SiO_4 , *Am. Mineral.* 100 (2015) 1736–1743. <https://doi.org/10.2138/am-2015-4744>.

Spivak A.V., Litvin Yu.A., Zakharchenko E.S. Formation and stability of ahrensite γ -Fe₂SiO₄ at 15-20 GPa UDC 549.01

IEM RAS, Chernogolovka (spivak@iem.ac.ru)

Abstract. A series of experiments was carried out to study phase relations within the polythermal section (Mg₂SiO₄)₇₀(Carb*)₃₀ - (Fe₂SiO₄)₇₀(Carb*)₃₀ of the Mg₂SiO₄ - Fe₂SiO₄ - CaCO₃ - Na₂CO₃ - K₂CO₃ system at 15-20 GPa. Experimental data were obtained on the conditions of formation and stability of ahrensite, as well as on phase reactions in a diamond-forming system enriched with an iron component Fe₂SiO₄.

Keywords: transition zone, diamond-forming systems, melting relations, HPHT experiment, high pressures, ahrensite, ringwoodite

Determining the phase and chemical composition of the Earth's transition zone and the lower mantle is a fundamental problem in Earth science. According to experimental and theoretical data, Fe-containing wadsleyite, ringwoodite (Mg,Fe)₂SiO₄ and bridgmanite (Mg,Fe)(Si,Al)O₃ are the main minerals of the deep horizons of the Earth. These minerals are also found among inclusions in deep diamonds together with ferropericlase, stishovite, and other high-pressure minerals.

Ahrensite (γ -Fe₂SiO₄) is iron analog (#Mg<50) of silicate-spinel ringwoodite (γ -Mg₂SiO₄), has been discovered in meteorite (Ma et al., 2016). The Earth's mantle Fe-rich phases of (Fe,Mg)₂SiO₄ composition were found among diamond inclusions (Kaminsky, 2017). These grains in diamonds from placer deposits of the Juina area in Brazil have wide variations including low-Mg varieties (#Mg=88–89). More Fe-rich (#Mg=79) mineral phase (Fe,Mg)₂SiO₄ was identified as a single inclusion in diamond from the South African pipe, Jagersfontein (Chinn et al., 1998). In addition, ringwoodite (#Mg=75) with olivine and Ca-walstromite were found as an inclusion in diamond from the Juina, Brazil (Pearson et al., 2014).

Similar finds of iron-rich ringwoodite suggest that ferruginous varieties may form at the Earth's mantle conditions. Obtaining new experimental information on the effect of composition on stability of mantle phases will allow approaching a solution of the deep substance evolution problem. Crystal chemistry and stability of Fe-rich silicate, oxide and carbonate phases are critical for understanding structure, dynamics, and evolution of our planetary magmatism. In this regard, experimental studying of stability and reactionary interaction of ahrensite, ferruginous variety of ringwoodite with carbonate-containing melts becomes necessary in order to understand the processes of genesis of the mantle

rocks and minerals, and, in particular, diamond formation at the conditions of the transition zone of the Earth.

Experiments were carried out to study phase relations within the polythermal section (Mg₂SiO₄)₇₀(Carb*)₃₀ - (Fe₂SiO₄)₇₀(Carb*)₃₀ of the Mg₂SiO₄-Fe₂SiO₄-CaCO₃-Na₂CO₃-K₂CO₃ system at 15-20 GPa. Experimental data on conditions of formation and stability of ahrensite, on phase reactions in diamond-forming system enriched with iron component Fe₂SiO₄ were obtained.

Experiment on study of formation and stability of ahrensite and phase relations in the FeO-MgO-SiO₂-CaO-Na₂O-K₂O-CO₂ system was carried out at pressure 15-20 GPa and temperature 800-1900°C at the Bayerisches Geoinstitut (Bayreuth, Germany). The starting materials were homogeneous gel mixtures of Mg₂SiO₄, Fe₂SiO₄ and powdered mixture chemically pure carbonates CaCO₃, Na₂CO₃ and K₂CO₃ of boundary compositions of the polythermal section (Mg₂SiO₄)₇₀(Carb*)₃₀ - (Fe₂SiO₄)₇₀(Carb*)₃₀: (A) [(Mg₂SiO₄)₄₀(Fe₂SiO₄)₆₀]₇₀(Carb*)₃₀; (B) [(Mg₂SiO₄)₈₀(Fe₂SiO₄)₂₀]₇₀(Carb*)₃₀; (C) [(Mg₂SiO₄)₉₅(Fe₂SiO₄)₅]₇₀(Carb*)₃₀, where Carb* - CaCO₃ - 34, Na₂CO₃ - 33, K₂CO₃ - 33 (wt. %). Finally, a mixture was dried at 100 °C for 24 hours. A starting material was placed into a platinum capsule. A standard 10/5, 10/4 and 7/3 cell assemblages were used. The capsule was insulated from the heater by an MgO cylinder. High temperature was generated using a LaCrO₃ heater and a quenching procedure was applied. The accuracies of pressure and temperature determinations were estimated as ±0.5 GPa and ±50°C, respectively.

The chemical compositions of experimental samples were determined by electron microprobe analysis (EMPA) with using Tescan - VegaIIXMU electron microscopy with INCA Energy 450 energy dispersive spectrometer (EDS), equipped with an INCA x-sight semiconductor Si(Li) detector and an INCA Wave 700 wavelength-dispersive spectrometer (WDS) (Oxford Instruments) at IEM RAS. The microprobe measurements were carried out at an accelerating voltage 20 kV, a focused beam current of ~10 nA, and counting times of 60 - 120 s. For each phase, 7-10 analyzed points were measured and averaged.

Raman spectra of the experimental samples were measured in geometry of backscattering on an Acton SpectraPro-2500i spectrograph with a detector cooling up to -70 °C CCD Pixis2K and an Olympus microscope with continuous solid-state monomeric laser with a radiation wave-length of 532 nm and diode pumping at IEM RAS.

Table 1. Compositions of representative experimental phases of ringwoodite and ahrensite

phase	Rwd	Ahr*	Rwd	Ahr*	Ahr	Ahr*	Rwd	Rwd*
starting composition	A			B	B	C	B	
P, GPa	15				17		20	
T, °C	1400	1400	1500	1600	1500	1600	1500	1600
SiO ₂	34,19	31,05	34,91	30,21	30,48	23,99	34,78	34,42
FeO	35,00	45,32	37,32	48,20	54,90	72,18	33,02	34,73
MgO	29,76	22,63	28,09	19,46	14,16	3,80	31,40	27,02
CaO	n.f.	0,42	n.f.	0,40	0,06	n.f.	0,49	1,55
Na ₂ O	0,17	0,33	n.f.	0,45	0,28	n.f.	0,23	0,95
K ₂ O	n.f.	0,21	n.f.	0,98	0,10	n.f.	0,36	1,32
Sum	99,11	99,97	100,32	99,70	99,92	99,98	100,28	99,99
#Mg	60,21	47,15	57,29	41,89	31,56	8,55	62,83	58,24
Formula units for 4 oxygen atoms								
Si	0,89	0,86	0,91	0,86	0,92	0,79	0,89	0,90
Fe	0,77	1,05	0,81	1,15	1,33	2,00	0,71	0,76
Mg	1,16	0,94	1,09	0,83	0,61	0,19	1,20	1,06
Ca	-	0,01	-	0,01	-	-	0,01	0,04
Na	0,01	0,02	-	0,02	0,02	-	0,01	0,05
K	-	0,01	-	0,04	-	-	0,01	0,04
Sum	2,83	2,88	2,80	2,91	2,89	2,98	2,83	2,85

* - quenching phase

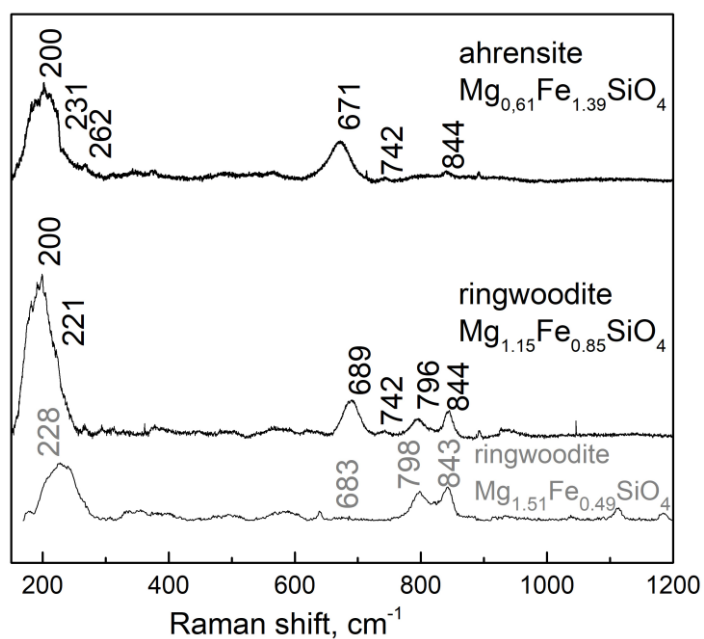


Fig. 1. Raman spectra of experimental samples of ringwoodite and ahrensite (black lines) in comparison with the Raman spectrum of ringwoodite from the database ruff # 070079 (gray line).

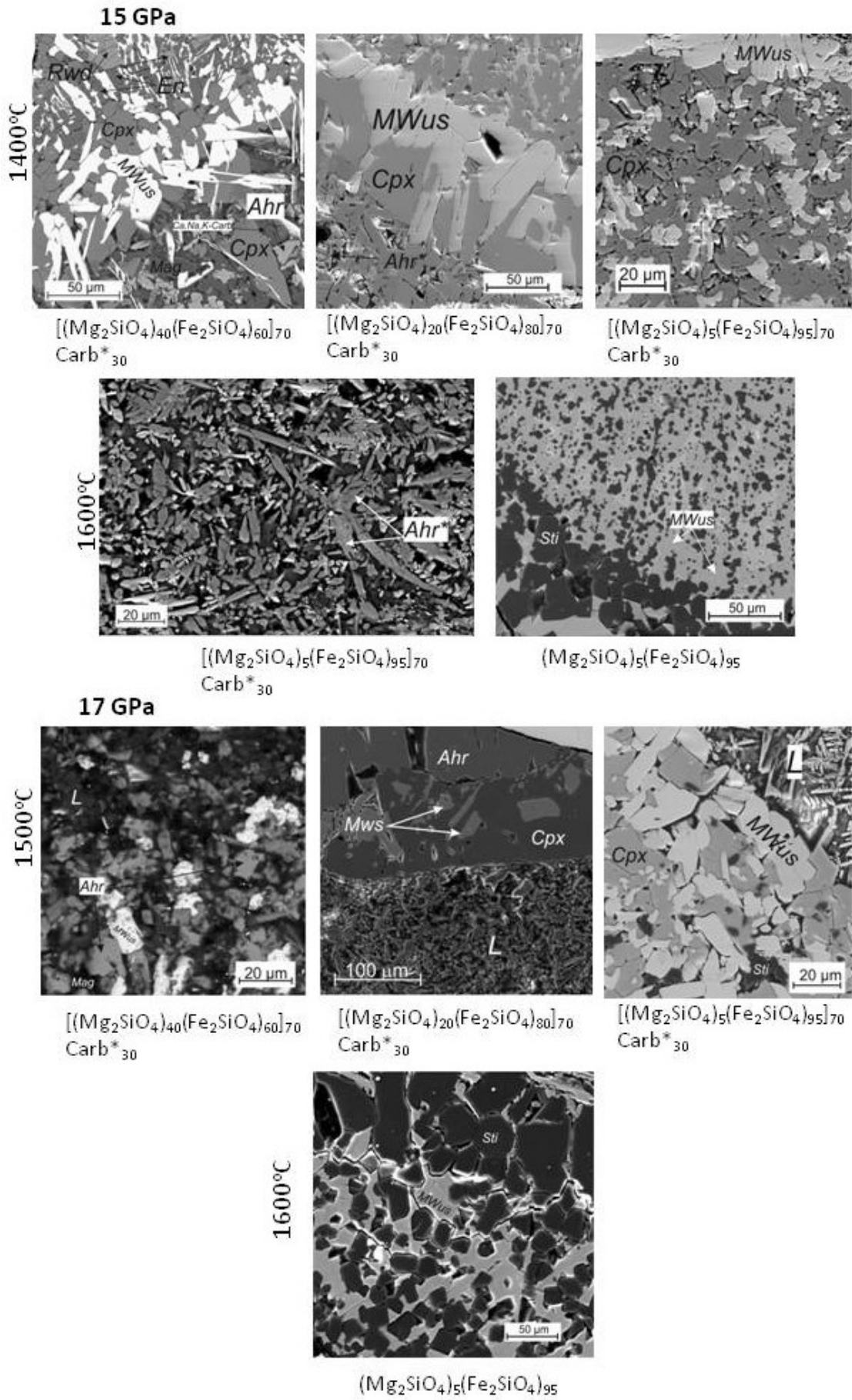


Fig. 2. SEM images of experimental samples for studying phase relations in carbonate-silicate and silicate systems at 15, 17 GPa

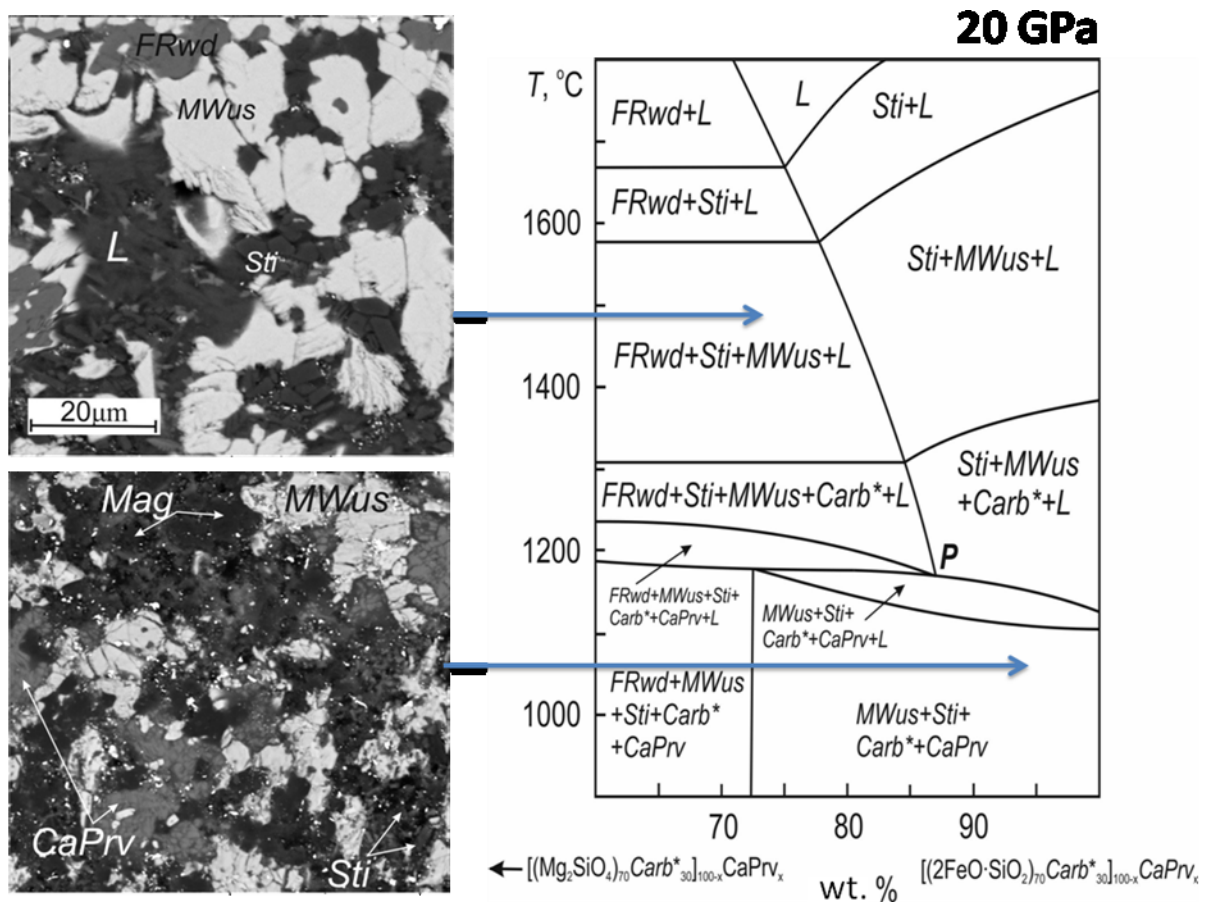


Fig. 3. Melting phase relations of the polythermal section $[(\text{Mg}_2\text{SiO}_4)_{70}\text{Carb}^*_{30}]_{100-x}\text{CaPrv}_x - [(\text{Fe}_2\text{O}\cdot\text{SiO}_2)_{70}\text{Carb}^*_{30}]_{100-x}\text{CaPrv}_x$ at 20 GPa.

In experimental samples at 15, 17 and 20 GPa and temperatures of 800-1900 °C the following phases were established: olivine, wadsleyite, ringwoodite (ahrensite is an iron-bearing variety of ringwoodite), enstatite, clinopyroxenes (augite, pigeonite), Ca-perovskite, magnesiowustite, carbonates (magnesite, Ca- and Fe- magnesite, Ca, Na, K-carbonates), melt. Structure and extent of crystallization of the experiment products depend on temperature and starting composition. Ahrensite crystals were formed at 17 GPa, 1500 °C using the starting composition $(\text{B})[(\text{Mg}_2\text{SiO}_4)_{80}(\text{Fe}_2\text{SiO}_4)_{20}]_{70}(\text{Carb}^*)_{30}$ and as the quenching phase for the composition (C) $[(\text{Mg}_2\text{SiO}_4)_{95}(\text{Fe}_2\text{SiO}_4)_5]_{70}(\text{Carb}^*)_{30}$ (Table 1, Fig. 1, 2). At 15 GPa, ahrensite crystallizes only as a quenching phase. At 20 GPa, ahrensite was not detected. Ringwoodite ($\#\text{Mg}=58-63$) was formed with using the starting composition B. With ferrous component increasing in the system (starting composition C), ringwoodite decomposed into magnesiowustite and stishovite. In test experiments at 15 and 17 GPa with the composition $(\text{Mg}_2\text{SiO}_4)_{95}(\text{Fe}_2\text{SiO}_4)_5$ the phase of $(\text{Mg,Fe})_2\text{SiO}_4$ composition was not detected, the association "magnesiowustite + stishovite" formed (Fig. 2).

Melting phase relations of the multicomponent silicate-carbonate system in its polythermal section $(\text{Mg}_2\text{SiO}_4)_{70}(\text{Carb}^*)_{30} - (\text{Fe}_2\text{SiO}_4)_{70}(\text{Carb}^*)_{30}$ have been studied experimentally at 15, 17, and 20 GPa and 800-1900 °C. The appearance of clinopyroxene in the system at 15 and 17 GPa and Ca-perovskite at 20 GPa as independent boundary phases is associated with the accompanying metasomatic interaction of Ca-carbonate and iron-bearing (ahrensite Fe_2SiO_4) components of the system. The content of iron component of starting compositions affect to magnesian content of ahrensite / ringwoodite, which ranges $\#\text{Mg}=31-66$. At 20 GPa the peritectic reaction of ringwoodite $(\text{Mg,Fe})_2\text{SiO}_4$ and melt was discovered with formation of the association of magnesiowustite $(\text{Mg,Fe})\text{O}$ and stishovite SiO_2 (Spivak et al., 2019). This reveals the physicochemical mechanism, which, combined with fractional crystallization regime, controls ultrabasic-basic evolution of magmatic and diamond-forming systems of the transition zone.

This work is fulfilled under the Research Program AAAA-A18-118020590140-7 of the Korzhinskii Institute of Experimental Mineralogy RAS.

References

- Kaminsky F. (2012) Mineralogy of the lower mantle: A review of “super-deep” mineral inclusions in diamond. *Earth-Science Rev.* **110**, 127–147.
- Ma C., Tschauer O., Beckett J. R., Liu Y., Rossman G. R., Sinogeikin S. V, Smith J. S. and Taylor L. A. (2016) Ahrensite, γ -Fe₂SiO₄, a new shock-metamorphic mineral from the Tissint meteorite: Implications for the Tissint shock event on Mars. *Geochim. Cosmochim. Acta* **184**, 240–256. Available at: <http://dx.doi.org/10.1016/j.gca.2016.04.042>.
- Pearson D. G., Brenker F. E., Nestola F., McNeill J., Nasdala L., Hutchison M. T., Matveev S., Mather K., Silversmit G., Schmitz S., Vekemans B. and Vincze L. (2014) Hydrous mantle transition zone indicated by ringwoodite included within diamond. *Nature* **507**, 221–224.
- Chinn, I.T., Milledge, H.J. & Gurney, J.J. (1998): Diamond and inclusions from the Jagersfontein kimberlite. In Seventh Int. Kimberlite Conf. (Cape Town), Extended Abstr., 156-157.
- Spivak A.V., Litvin Yu A., Zakharchenko E.S., Simonova D.A., Dubrovinsky L.S. (2019) Evolution of Diamond-Forming Systems of the Mantle Transition Zone: Ringwoodite Peritectic Reaction (Mg,Fe)₂SiO₄ (Experiment at 20 GPa). *Geochemistry International* **57**, № 9, 1000-1007.